UNIVERSITÀ DEGLI STUDI DI PADOVA

DIPARTIMENTO DI MEDICINA - DIMED

DOTTORATO DI RICERCA INTERNAZIONALE IN IPERTENSIONE ARTERIOSA E BIOLOGIA VASCOLARE

CICLO: XXVI

PREVALENCE OF KCNJ5 MUTATIONS AND FUNCTIONAL IMPACT OF A NOVEL KCNJ5-insT149 MUTATION IN ALDOSTERONE PRODUCING ADENOMA CAUSING RESISTANT HYPERTENSION

Coordinatore: Ch.mo Prof. Gian Paolo Rossi

Supervisore: Ch.ma Prof.ssa Teresa Maria Seccia

Dottorando: Dott. Maniselvan Kuppusamy

ANNO ACCADEMICO: 2013/2014

CONTENTS

S.NO	TITLE	PAGE NO.
1	ABSTRACT	5
2	INTRODUCTION	9
3	AIMS	22
4	MATERIALS AND METHODS	24
5	RESULTS	34
6	DISCUSSION	51
7	CONCLUSIONS AND PERSPECTIVES	56
8	REFERENCES	58

LIST OF ABBREVIATIONS

APA	-	Aldosterone producing adenoma
ATPase	-	Adenosine triphosphatase
Ca^{2+}	-	Calcium ion
cAMP	-	Cyclic adenosine monophosphate
cDNA	-	Complementary DNA
CVD	-	Cardio vascular diseases
CYP11B1	-	Cytochrome P450 family 11 subfamily B polypeptide 1
CYP11B2	-	Cytochrome P450 family 11 subfamily B polypeptide 2
DAB	-	3, 3'-diaminobenzidine tetra hydrochloride
GIRK	-	G protein-coupled inwardly-rectifying potassium channels
HBP	-	High blood pressure
HT	-	Hypertension
K^+	-	Potassium
KCNJ5	-	Potassium inwardly-rectifying channel subfamily J member 5
Na^+	-	Sodium
$NMDG^+$	-	N-methyl-d-glucamine
PA	-	Primary aldosteronism
PBGD	-	Porphobilinogen deaminase
PBS	-	Phosphate buffered saline
PCR	-	Polymerase chain reaction
pH	-	Hydrogen ion concentration
qRT-PCR	-	Quantitative real time-PCR
RNA	-	Ribonucleic acid
RT-PCR	-	Reverse transcriptase-polymerase chain reaction
SDM	-	Site directed mutagenesis

RIASSUNTO

L' iperaldosteronismo primario (PA) è la causa più frequente di ipertensione secondaria ed è caratterizzato da una secrezione elevata ed autonoma di aldosterone. Le due forme principali sono l'iperplasia surrenalica bilaterale e l'adenoma secernente aldosterone. I meccanismi molecolari alla base dell'ipersecrezione di aldosterone sono tuttora sconosciuti.

Tuttavia recenti studi hanno dimostrato che sostituzioni amminoacidiche all'interno del filtro di selettività del canale del potassio Kir3.4 (KCNJ5 possono provocare una secrezione autonoma di aldosterone in adenomi producenti aldosterone (APA). Tali mutazioni somatiche sono associate ad alti livelli plasmatici di aldosterone nei pazienti con APA, suggerendo un ruolo causale di tali mutazioni nello sviluppo di APA e iperaldosteronismo. Pertanto abbiamo condotto uno studio in pazienti affetti da APA afferenti a due centri di riferimento italiani, effettuando lo screening per le mutazioni somatiche di KCNJ5, ed abbiamo individuato e caratterizzato la mutazione KCNJ5-insT149, mai descritta in precedenza.

Mediante analisi ad alta risoluzione delle curve di melting per le mutazioni in KCNJ5 sono stati studiati 195 pazienti consecutive con una diagnosi conclusiva di APA. Il 24,6% dei pazienti presentava una mutazione nel filtro di selettività del KCNJ5, tale prevalenza è stata confermata mediante sequenziamento Sanger.

Nei pazienti affetti da mutazione di KCNJ5 l'espressione genica di CYP11B2 (29,9 ± 7,4 vs 10,3 ± 3,6, P <0,02), ma non quella di CYP11B1, risultava superiore rispetto ai pazienti non affetti da mutazioni, lo stesso valeva per l'indice di lateralizzazione.

In un paziente con ipertensione farmaco-resistente grave è stata identificata l' inserzione c.446insAAC, che codifica per la proteina mutante KCNJ5-insT149. Per caratterizzare funzionalmente questa nuova mutazione, attaverso mutagenesi sito-diretta, è stato generato un cDNA codificante per il canale KCNJ5 mutato e trasfettato in cellule di mammifero. Il cDNA codificante KCNJ3 è stato transfettato insieme a quello per KCNJ5 in modo da riprodurre la struttura tetramerica del canale KCNJ3/KCNJ5.

CYP11B1, CYP11B2 e 17α-idrossilasi sono stati rilevati attraverso tecniche di immunoistochimica e immunofluorescenza nella ghiandola surrenale del paziente. L'espressione genica di CYP11B2 e le concentrazioni di aldosterone sono stati misurati per studiare l'impatto della mutazione sull'attività secernente. Utilizzando la tecnica di "whole-cell patch clamp e modeling molecolare" abbiamo studiato le correnti trans-membrana di Na^+ e Ca^{2+} e generato una immagine 3D del canale insT149 KCNJ5. Rispetto al wild type e alle cellule adrenocorticali HAC15, le cellule transfettate con KCNJ5-insT149 esprimevano alti livelli del gene CYP11B2 e mostravano un'aumentata produzione di aldosterone.

Allo stesso modo cellule HEK293 che esprimono il canale KCNJ5-insT149 mutato mostravano un aumento pari a due volte di Na^+ intracellulare e un aumento sostanziale di Ca^{2+} intracellulare in seguito all' attivazione dei canali del Ca^{2+} voltaggio-dipendenti. Quindi, la nuova mutazione del canale del K^+ KCNJ5 induce un'anomala permeabilità della membrana al Na^+, depolarizzazione della membrana, un aumento di Ca^{2+} intracellulare e aumento della sintesi di aldosterone.

I nostri risultati nel complesso supportano il concetto che le canalopatie che coinvolgono il canale del K^+ KCNJ5 sono alla base della secrezione costitutiva di aldosterone in pazienti affetti da APA.

ABSTRACT

Primary aldosteronism (PA), a common form of secondary hypertension, is characterized by an excess autonomous aldosterone secretion. In a percentage ranging from a half to two thirds of the cases it is due to a surgically curable aldosterone-producing adenoma (APA) and in the rest to bilateral adrenal hyperplasia. The molecular mechanisms underlying aldosterone hypersecretion are unknown.

Recent evidences suggest that amino acid residue substitutions in the selectivity filter of the Kir3.4 (KCNJ5) potassium channel may cause a constitutive aldosterone secretion from aldosterone-producing adenomas (APA). Such somatic mutations were also found to be associated with higher plasma aldosterone concentrations in the patients with an APA, thereby suggesting a causative role of the mutations in the development of APA and hyperaldosteronism. Hence, we performed a study with the aims to search for KCNJ5 mutations in APA patients referred to two Italian referral centers. Through this search we could also identify a novel KCNJ5-insT149 mutation out of the selectivity filter that was a fully characterized from the electrophysiological and phenotypic standpoint.

APA samples (n=195) from consecutive patients with a conclusive diagnosis of APA were screened by high melting resolution curve for KCNJ5 mutations. We found that the mutations occurred in 24.6% of patients. These findings were confirmed by Sanger sequencing. The mRNA content of CYP11B2, but not of CYP11B1, and plasma aldosterone and, accordingly, the lateralization index were higher ($P < 0.02$) in the APA with the mutation than in the APA without such mutations.

A novel c.446insAAC insertion resulting in the mutant protein KCNJ5-insT149 was identified In a patient presenting with severe drug-resistant hypertension. To functionally characterize this novel KCNJ5 channel mutation a mutated cDNA harbouring c.446insAAC insertion was generated by site-directed mutagenesis and transfected in mammalian cells. KCNJ3 cDNA was also transfected into the same cells to reproduce the tetrameric structure of the KCNJ3/KCNJ5 channel.

CYP11B1, CYP11B2 and 17α-hydroxylase were localized in the adrenal gland of the mutated APA patient with immunohistochemistry and immunofluorescence.

CYP11B2 mRNA levels and aldosterone concentrations were also measured to investigate the impact of the mutation on the secreting activity. By using a whole-cell patch clamp technique and molecular modeling we explored membrane Na^+ and Ca^{2+} currents and created a 3D image of the insT149 KCNJ5 channel. Compared to wild type and mock-transfected HAC15 adrenocortical cells, those expressing the mutant KCNJ5 showed increased CYP11B2 expression and aldosterone secretion. Likewise HEK293 expressing the mutated KCNJ5-insT149 channel exhibited a 2-fold increase in intracellular Na^+ and a substantial rise in intracellular Ca^{2+} caused by activation of voltage-gated Ca^{2+} channels. Hence, the novel KCNJ5 K^+ channel mutation induces abnormal Na^+ permeability, membrane depolarization, a rise in cytosolic Ca^{2+} and increased aldosterone synthesis.

Thus, our findings support the concept that channelopathies involving the KCNJ5 K^+ channel mechanistically account for constitutive secretion of aldosterone in human APA.

INTRODUCTION

INTRODUCTION

The Global brief on hypertension*: silent killer, global public health crisis* describes why, in the early 21st century, arterial hypertension (HT) is still a global public health issue. It describes how hypertension contributes to the burden of heart disease, stroke, kidney failure and premature death and disability. The recent updates on CVDs statistics information shows that about 8% of death occurs as a results of high blood pressure in United States, and also that HT is a major cardiovascular risk factor that affects between 10 and 40% of the population in industrialized countries (WHO;, 1999).

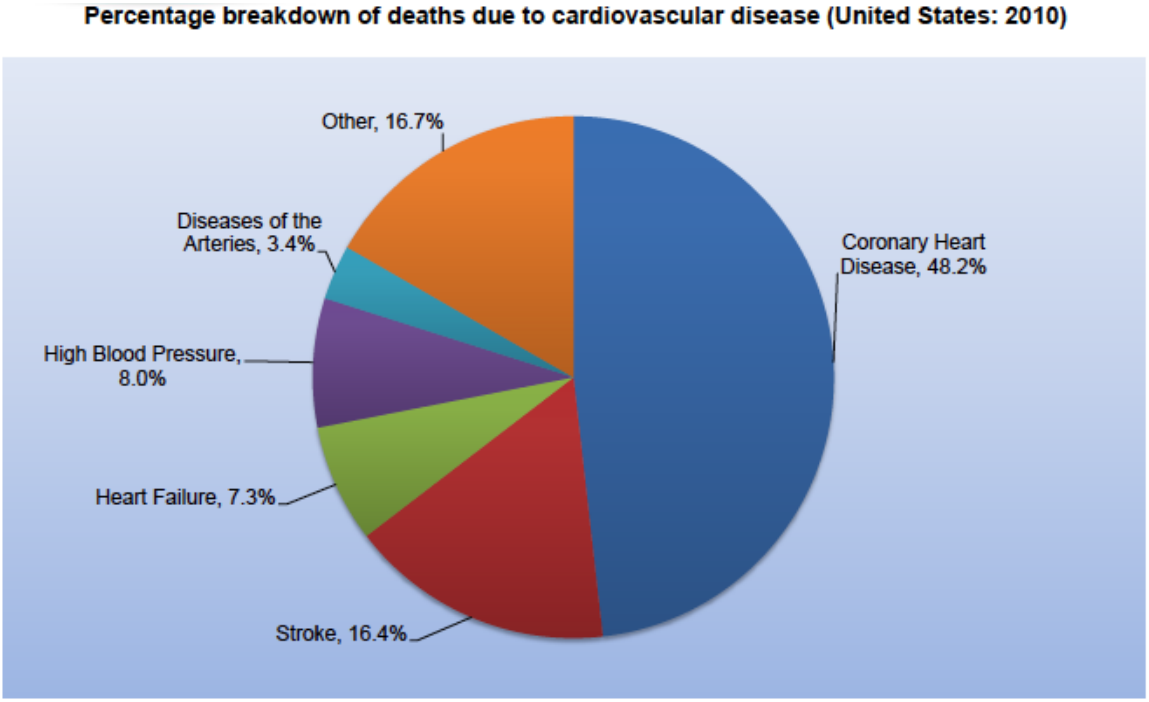

Primary aldosteronism

Primary aldosteronism (PA) is the most common endocrine disease cause of secondary hypertension and autonomous secretion of aldosterone. PA entails a variety of disorders characterized by an overproduction of aldosterone that is relatively independent of the renin-angiotensin-aldosterone system and is not suppressed with sodium overload. The overproduction of aldosterone causes suppression of plasma renin, high blood pressure values, sodium retention, increased potassium excretion leading to hypokalemia, and finally

cardiovascular damage. Prolonged exposure to high plasma aldosterone concentrations is associated with oxidative stress, cardiovascular remodeling, hypertrophy, and fibrosis in a process that is independent of arterial blood pressure (BP) values.

The biochemical pattern of PA can be caused by Idiopathic hyperplasia, bilateral (BAH, 60-65%) or unilateral (UAH, 2-3%), aldosterone-producing adenoma (APA, 30-35%), aldosterone-producing adrenocortical carcinoma (< 1%), glucocorticoid-remediable aldosteronism (GRA) (familial hyperaldosteronism (FH) type I, < 1%), Familial hyperaldosteronism (FH type II, APA, or IHA) < 1%, Familial hyperaldosteronism (FH type III) < 1% and ectopic aldosterone-producing adenoma or carcinoma < 1% (Rayner, 2008; Stowasser & Gordon, 2013).

The familiar form GRA is characterized by early-onset, severe hypertension, refractory to conventional antihypertensive medications. The underlying mutation is a chimeric gene duplication resulting from unequal crossing-over between the promoter sequences of 11-β hydroxylase (CYP11B1), which is responsive to corticotrophin stimulation, and coding sequences of aldosterone synthase (CYP11B2), both on chromosome 8. An autosomal dominantly inherited disorder; this leads to ACTH-sensitive aldosterone overproduction. The main features consist of increased aldosterone and hybrid steroid products (18-OH-cortisol and 18-oxo-cortisol), which are suppressible with exogenous corticosteroid (Geller et al, 2008; Richard P et al, 1992).

FH type II is an autosomal dominantly inherited, genetically heterogeneous disorder. FH type II families can present clinically with APA or IHA, and are not distinguishable from patients with non-familial PA. The exact prevalence of FH type II is not known, but there are case series reporting a high percentage of affected patients (7%). FH type II is more common than GRA, and is reportedly linked to chromosome 7p22 (So et al, 2005).

FH type III is a newly discovered clinical entity. First described by Geller and co-workers (Geller et al, 2008), it is a particularly aggressive form of hyperaldosteronism, with medication-resistant hypertension. The genetic cause of this syndrome appears to be inherited germline mutations in KCNJ5, which encodes the potassium channel Kir3.4. (Choi

et al, 2011). This germline mutation could cause the loss of channel selectivity for potassium and increased sodium conductance, which leads to depolarization of zona-glomerulosa cells. Depolarization activates voltage- gated Ca^{2+} channels with intracellular Ca^{2+} rising, inducing aldosterone production. Chronic Ca^{2+} stimulation also promotes zona-glomerulosa cellular proliferation. Clinically patients with FH type III present with severe hypertension and variable hypokalemia, with radiological bilateral massive adrenal hyperplasia.

BAH or APA are the most common form of PA that accounting for more than 90% of clinical cases (Rayner, 2008). Unilateral adrenal hyperplasia is less commonly identified and only 1% of PA patients have aldosterone-producing carcinoma, with 10% of them showing metastasis at diagnosis (Seccia et al, 2005).

Although PA has long been considered a rare cause of hypertension, numerous studies performed in recent years have reported an increase in the prevalence of PA. The largest study on Primary Aldosteronism Prevalence in Italy (PAPY), a prospective survey of 1180 consecutive newly diagnosed hypertensive patients referred to specialized hypertension centers, APA and IHA were found in 4.8% and 6.4% of all patients, respectively, thus leading to an overall prevalence of PA of 11.2% (Rossi et al, 2006a). Clinically, the distinction between the major causes of PA is crucial for the choice of treatment. While the treatment indicated for APAs is surgical removal, the treatment of choice for IAH is medical therapy with mineralocorticoid receptor antagonists (Rossi et al, 2008).

The first case of PA was reported by Litynski (Litynski, 1953), but Conn was the first to well characterize the disorder in 1956. PA, described by Conn in a 34-year-old woman, was characterized by hypertension, intermittent paralysis, hypokalemia and metabolic alkalosis. Further biochemical analyses detected increased activity of urinary salt-retaining corticoid hormone. The patient was cured by removal of a benign adrenal adenoma (Conn & Louis, 1956).

The diagnosis of APA, the unique clinical form of PA identifiable with certainty, is established when the following stringent “four corners” criteria are satisfied: (1) biochemical evidence of PA; (2) lateralization of aldosterone secretion at AVS or at ^{131}**I**-

norcholesterol dexamethasone–suppressed adrenocortical scintigraphy; (3) evidence of adenoma at computed tomography, and/or magnetic resonance, and/or surgery, and/or pathology; (4) demonstration of normokalemia and HT cure, or improvement, at follow-up after adrenalectomy (Rossi et al, 2006a; Rossi et al, 2006b).

Pathophysiology of aldosterone secretion

The important pathophysiologic anomaly causing PA syndrome is the autonomous aldosterone production. The steroid hormone aldosterone, secreted by the glomerulosa cells of zona glomerulosa region in the adrenal cortex, controls sodium and potassium balance, and also influences acid-base homeostasis of the vertebrate organism. The main physiological targets are the epithelial cells, mostly located in the distal nephron. It enhances Na^+ reabsorption as well as K^+ and H^+ excretion. Sodium retention promotes water retention, with expansion of the extracellular volume, hypertension, and suppression of renin production (Rossi et al, 2006b). Excessive potassium loss causes hypokalemic alkalosis, which may be associated with various clinical features, varying from abnormal electrocardiographic findings up to muscular weakness and tetany. In past years, hypokalemia was thought to be a hallmark of primary aldosteronism, but noted by Conn and colleagues as early as in 1965 (Conn, 1955), potassium levels in primary aldosteronism could also be normal. Moreover, more recent studies confirmed that most patients with PA are normokalemic (Calhoun et al, 2008; Mulatero et al, 2004; Rossi et al, 2002).

In addition to its epithelial actions, aldosterone has some effects on non-epithelial tissues. These include increased oxidative stress and collagen remodeling, resulting in endothelial dysfunction, left ventricular hypertrophy and fibrosis in the kidney, heart and blood vessels (Brown, 2005).

Molecular mechanisms underlying excess aldosterone production

The genetic background of APA and the molecular mechanisms by which a normal adrenocortical zona glomerulosa evolves into an aldosteronoma causing autonomous higher secretion of aldosterone remain poorly understood. The most obvious candidate gene, CYP11B2, does not participate in tumorigenesis in most adrenocortical lesions: only in

familial hyperaldosteronism type I there is an aberrant expression of the CYP11B2 gene (fusion between the corticotrophin-regulated promoter of 11-β–hydroxylase and the sequence that codes for aldosterone synthase) (Richard P et al, 1992). Microarray analysis and quantitative RT-PCR, the expression profiles of the steroidogenic enzymes in APA and normal adrenal cortex demonstrated an overexpression of CYP11B2, 11ß-hydroxysteroid dehydrogenase type 2 (HSD11B2) and CYP21 (21-hydroxylase). They also examined, in adenoma samples, the presence/absence of SF-1 and DAX-1 that are known as two orphan receptors co-localized in the adrenal gland and are implicated in the transcriptional regulation of several steroidogenic genes, including StAR, CYP11A, CYP17, and CYP11B2. The study highlighted that mRNA levels for both SF-1 and DAX-1 were higher in APA than in normal adrenal cortex (Bassett et al, 2005).

Recent finding shows that transcriptome profiling analysis and quantitative RT-PCR compared the whole transcriptome of APAs with a pool of histologically normal sub capsular adrenocortical tissues. Based on steroidogenic enzyme gene expression profiles, two APA subgroups were identified: featuring overexpression of CYP11B2, CAMK-I, 11-β-hydroxylase, 3-β-hydroxysteroid dehydrogenase, and 21-hydroxylase and under expression of CAMK-II B and the other one with an opposite profile. The low CYP11B2 group exhibited a longer known duration of hypertension and a lower rate of long-term cure; instead, the high CYP11B2 patients had a significantly shorter known duration of hypertension (Lenzini et al, 2007; Wang et al, 2011). This study suggested that aldosterone overproduction in APAs involves complex alterations of aldosterone synthesis regulation rather than simply increased aldosterone synthase gene expression. In fact, a transcriptome analysis of APA compared with adjacent adrenal gland showed several novel genes that are associated with APA phenotype.

Potassium channels in the Adrenal gland

Potassium channels mainly regulate the membrane voltage of aldosterone-producing glomerulosa cells in the adrenal glands. The secretion of aldosterone is controlled by the electrical potential of adrenal glomerulosa cells. Adrenal glomerulosa cells are uniquely sensitive to small increases in an extracellular K^+ levels because of the presence of very high

background K^+ conductance, which makes the membrane potential strictly dependent on the K^+ equilibrium potential. In humans, Volume depletion activates the renin-angiotensin system, producing the hormone angiotensin II (Ang II), which signals via its G protein–coupled receptor (GPCR) in glomerulosa cells. The resting membrane potential is set by K^+ channel activity; both Ang II signaling and hyperkalemia cause membrane depolarization and activation of voltage-gated Ca^{2+} channels. The glomerulosa cell is certainly the cell type most sensitive to extracellular K^+ in the mammalian organism. K^+ is a powerful stimulus of aldosterone production by incubated glomerulosa cells, and raising K^+ concentration ($[K^+]$) by a mere 1 mM already doubles the hormone production. Generally, the effect of K+ is mediated by Ca^{2+} influx (Spät, 2004).

Adrenal glomerulosa cells normally hyperpolarized because of a predominant K^+ conductance, primarily mediated by 'leak' K^+ channels of the K_2P family, TASK1 (TWIK-related acid-sensitive K(+) channel 1), TASK3 (TWIK-related acid-sensitive K(+) channel 3), and TREK1 (Tandem pore domain potassium channel 1), etc,.(Scholl & Lifton, 2013). Several K^+ channels show high levels of expression in the adrenal cortex and are believed to be important for the control of hormone secretion, e.g. KCNJ5, TASK1, TASK2, TASK3, KCNMA1, and KCNQ1. In considering with all leak and inward rectifying potassium channels TASK1, TASK2 and TASK3 and inward rectifying GIRK channels are central attentions on PA.

In adrenal glomerulosa cells several studies showed that TASK1 alone or TASK1/TASK3 knockout mouse mimics the PA (Heitzmann et al, 2008; Lucinda A et al, 2008). The expression of two members of the KCNK family, TASK3 (KCNK9) and TREK1 (KNCK2), in H295R cells suggested to have a role in setting the membrane potential in these cells; however, the production of aldosterone was not significantly altered by dominant-negative TASK3 or TREK1 (Brenner & Shaughnessy, 2008).

More recent findings from our group revealed lower expression of the TASK2 gene is a hallmark of APA causing human primary aldosteronism (Lenzini et al, 2013) and is associated to an increased expression of StAR, CYP11B2, hsa-miR-23 and hsa-miR-34, along an enhanced production of aldosterone in vitro, thereby providing a possible explanation for hyperaldosteronism in APA in spite of the suppression of angiotensin II, the

hypertension and the hypokalemia.

G protein-activated inward rectifier potassium channel 4

Inwardly rectifying potassium channels (IRK or Kir) are a specific subset of potassium selective ion channels that passes current (positive charge) more often in the inward direction (into the cell) than in the outward direction. Four G protein-activated IRK channel (GIRK) channel subunits (GIRK1-GIRK4) have been identified in mammals. They have diverse physiological functions depending on their type and their location. These GIRK are regulated by G protein-coupled receptors, which is widely expressed in physiological system including cardiac myocytes, neurons, endothelial cells, glial cells, epithelial cells and oocytes (Wickman et al, 2002). Functional GIRK channels are tetrameric assemblies of Kir3 family subunits. The assembly can be either homomeric or heteromeric forms. The mechanisms underlying rectification and its structural basis are similar to those that of other Kir channels. These K^+ channel consists two putative membrane-spanning domains and form tetrameric complexes linked by an extracellular pore-forming region and amino and carboxy-terminal domains. The selectivity filter is a conserved region within this family of channels that allows the selective trans- port of potassium over other cations (Hibino et al, 2010).

Kir3.4/GIRK4/CIR/KCNJ5 (potassium inwardly-rectifying channel, subfamily J, member 5) was first identified in bovine atrial membrane accompanied by Kir3.1 protein. The heterotetrameric assemblies of Kir3.4 and Kir3.1 expression stoichiometry of 1:1 ration were identified (Corey, 1998b). A homotetramer of Kir3.4 was also found in atrial myocytes, implying that Kir3.4 may form a homomer as well (Corey, 1998a). Acetylcholine induces activation of a specific population of K^+ channels, cardiac Kir3.X channels that are composed of Kir3.1 and Kir3.4 subunits (G et al, 1995). Kir3.4 knockout mice proved role of Kir3.X channels in the heart. In knockout mice atrial myocytes, no Kir3.X current (IKACh) was detected. Strikingly, the knockout mice lost heart rate variability, i.e., the beat-to-beat fluctuations determined by the balance between sympathetic and parasympathetic influences (Chun et al, 1994).

The amino-acid sequences from a range of ion channels show remarkable similarity in the

region of the selectivity filter. Red highlights show the conserved glycines in the signature sequence TVGYG, found in the potassium ion channel KcsA. Yellow highlights show amino acids that are chemically similar.

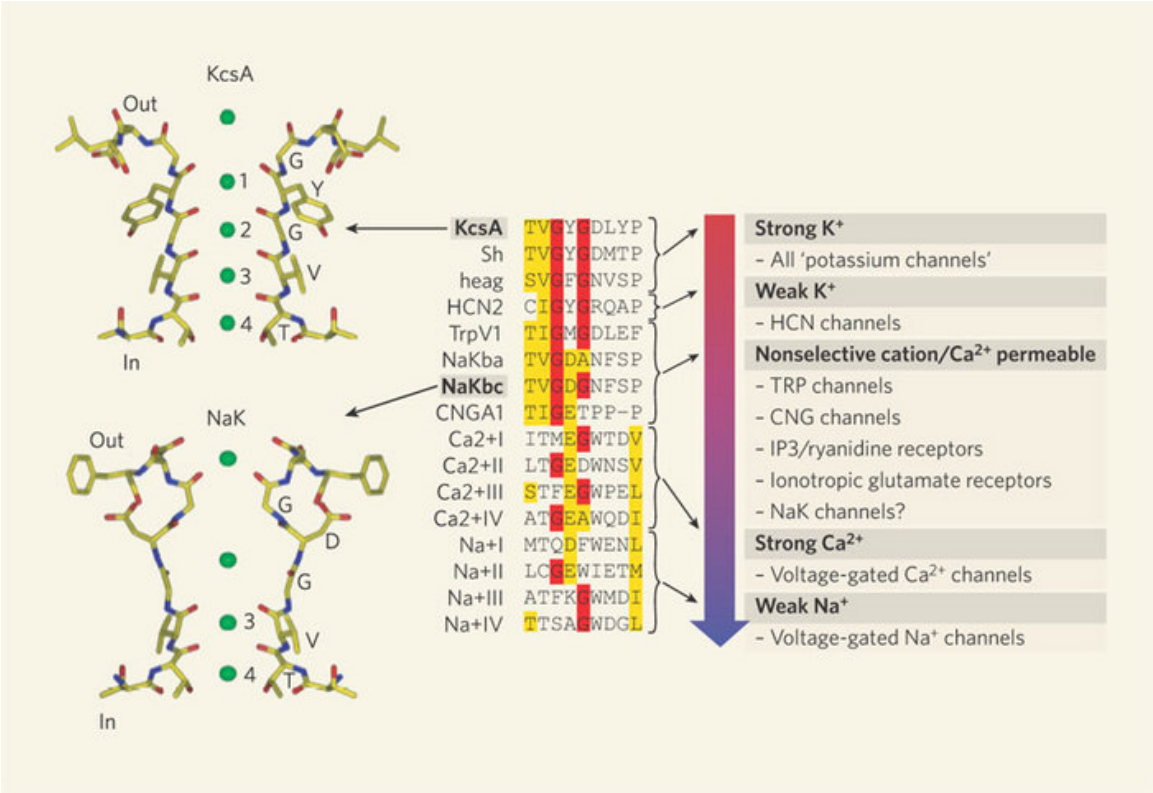

As the filter sequence becomes less conserved, the channels lose their selectivity for K^+ over Na^+ and become more permeable to Ca^{2+}. The structure of the non-selective cation channel NaK from Bacillus cereus has been solved and comparison of the selectivity filters of NaK and KcsA provides structural clues to sodium-ion permeability. Ion selectivity strong to week discrimination form was shown (Zagotta, 2006).

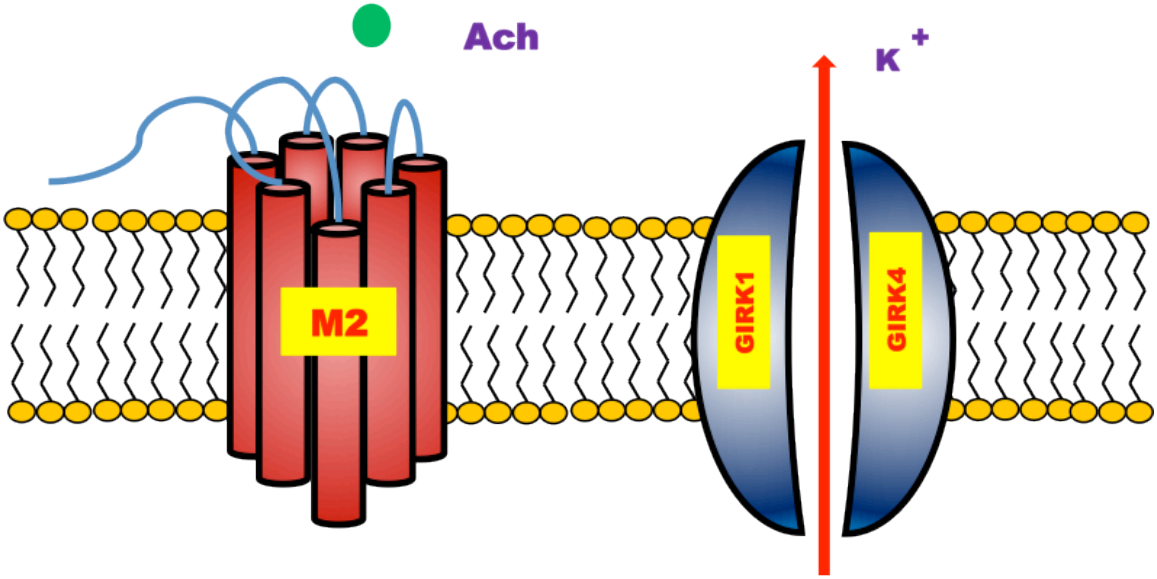

Moreover, GIRK potassium channel is most important in determining potassium flow and membrane polarization. These channels are mainly associated with obesity, LQTs syndrome and aldosterone synthesis.

Kir3.4 and associated diseases

Atrial fibrillation is common cardiac arrhythmia in clinical practice, which occurs in paroxysms, but can become persistent due to remodeling of atrial electrophysiology. IKACh has been found to play an important role in chronic atrial fibrillation and IKACh composed of Kir3.1/3.4 could be a therapeutic target for atrial fibrillation prevention and treatment. The changes in the electrical properties of atrial cardiomyocytes, such as a decrease of L-type Ca^{2+} current density and an increase of I_{K1} current density, are thought to contribute to the pathology of persistent atrial fibrillation (Dobrev et al, 2005). Recent report shown that 187 early-onset lone-AF patients had two SNPs in KCNJ5 (rs6590357 and rs7118824) that were found to be significantly associated with AF in Caucasians population (Jabbari et al, 2011). The study showed that implication of common variants in KCNJ5 rather than mutations in KCNJ2, KCNJ3 and KCNJ5 are associated with early-onset lone Atrial fibrillation.

Congenital long QT syndrome (LQTS) is a hereditary disorder that leads to sudden cardiac death secondary to fatal cardiac arrhythmias. Recently, the genetic locus of the LQTS-associated gene was mapped to chromosome 11q23.3-24.3. A heterozygous mutation (Kir3.4-Gly387Arg) was identified Kir3.4. The Kir3.4-Gly387Arg mutation was present in all nine affected family members and absent in 528 ethnically matched controls. Mutations in these genes have been identified in approximately 60-70% of the individuals affected with LQTS. Heterologous expression studies with Kir3.4-Gly387Arg revealed a loss-of-function electrophysiological phenotype resulting from reduced plasma membrane expression. These findings suggest mutation in Kir3.4 exerts dominant negative effects on Kir3.1/Kir3.4 channel complexes, linking it to congenital LQTS (Yang et al, 2010).

G protein-coupled inward rectifier K^+ channels 4 (GIRK4) gene expressions have been implicated also in the development of obesity, a key feature of metabolic syndrome. The entire GIRK4 gene, including all exons, the promoter and untranslated regions from 48 metabolic syndrome individuals was studied in order to identify genetic variations associated with the disorder. Targeted genotyping of four common single nucleotide polymorphisms (SNPs: rs11221497, rs6590357, rs4937391 and rs2604204) and one novel missense mutation (M210I) were found (Li et al, 2012). This finding gives hints that GIRK4 variants appears to associated with MetS in the Uygurian population, and this association may be influenced by age.

APA and G-protein-activated inward rectifier potassium channel 4 (GIRK4)

In a pioneering study by Lifton and co-workers have described somatic mutations of the K^+ channel KCNJ5 in aldosterone producing adenoma that advances in understanding of somatic gene mutations in APA and have uncovered several mutations in the selectivity filter of the G-protein-activated inward rectifying potassium channel Kir3.4, coded by the KCNJ5 gene (Choi et al, 2011). They reported two recurring mutations in or around the GYG motif in the KCNJ5 gene resulting in a marked change in selectivity for K^+ in comparison with sodium of the Kir3.4 channel in 8 of 22 patients studied. Mutations in and near K^+ channel selectivity filters can alter channel selectivity to produce nonselective cation channels.

The most common mutations validated in subsequent studies by multiple research groups

in different populations around the world are G151R in the narrow point of the filter and L168R, which might disrupt local salt bridge formation through the exordium of a positive charged amino acid (Gomez-Sanchez & Oki, 2013). About half patients with PA have APAs; 30%–70% of APA has somatic mutations of the selectivity filter of the G protein-activated inward rectifying potassium channel Kir3.4 coded by the KCNJ5 gene, with higher prevalence in women, and the highest prevalence found in Japan (Taguchi et al, 2012). Additional mutations in or surrounding the selectivity filter have been found, including R52H, E145Q, E145K, G151E, Y152C, I157C, delI157, T158A, E246K, G247R and E282Q (Akerstrom et al, 2012; Azizan et al, 2012; Azizan et al, 2013; Charmandari et al, 2012; Choi et al, 2011; Monticone et al, 2013; Murthy et al, 2013; Scholl et al, 2013). Hence, mutations showed gender dimorphism among the patients, being female and younger patients more prevalent than the male counterparts.

The T158A mutation was found in the germinal line of a family with hyperaldosteronism type 3 with a very severe hyperaldosteronism and hypertension requiring bilateral adrenalectomy for control of the hypertension and was associated with bilateral hyperplasia, not adenoma (Choi et al, 2011; Geller et al, 2008). The somatic mutation T158A was also found in 3 case of APA (Mulatero et al, 2012). G151E, Y152C, and I157C germinal mutations accounted for mild hyperaldosteronism, whereas T158A mutation identified a severe hyperaldosteronism (Charmandari et al, 2012; Monticone et al, 2012; Scholl et al, 2012).

Electrophysiological studies conducted in HEK-293T cell lines expressing wild type or mutant KCNJ5 (co-expressed with wild type KCNJ3) showed loss of selectivity of the KCNJ5/KCNJ3 channel and increased sodium permeability, resulting in continuous membrane depolarization. More recent studies have demonstrated that expression of mutant KCNJ5 in the adrenal cells causes depolarization, increased intracellular calcium, aldosterone production, and CYP11B2 expression (Gomez-Sanchez & Oki, 2013; Monticone et al, 2012).

Mutations in KCNJ5 selectivity filter also translated into changes in cell growth, thereby promoting proliferation of glomerulosa cells and clonal expansion. Moreover, the modified bee venom, tertiapin-Q, which is an inhibitor of Kir channels, abolished whole-cell currents,

but it could not affect such currents when KCNJ5 was mutated. The mutations, in fact, produced structural changes to the binding surface that markedly altered the affinity for tertiapin-Q (Murthy et al, 2012).

Recent findings from our group showed that APAs with KCNJ5 mutations have higher expression of the aldosterone synthase (CYP11B2) gene than those without such mutations. Moreover, the higher aldosterone secretion from the mutated APA into the adrenal vein paralleled a higher lateralization index than that found in the wild type patients. Thus, the presence or absence of KCNJ5 mutations can affect the accuracy of the AVS-based diagnosis in the patients with KCNJ5 mutations because they are more likely diagnosed and treated with adrenalectomy (Seccia et al, 2012).

Kir3.4 is primarily expressed in ZG in the adrenal gland, and its levels are high in the APA (Monticone et al, 2012). Data concerning the mutated APA were conflicting, with some studies showing lower Kir3.4 expression levels and others reporting higher levels (Boulkroun et al, 2012; Taguchi et al, 2012). Of interest, an increased expression of Kir3.4 was found in the tumoural nodules adjacent to the APA and ZG hyperplasia in patients with IHA (Monticone et al, 2012). More recently, new somatic mutations were identified in roughly 7% of APA (Beuschlein et al, 2013). Somatic mutations in the P-type adenosine triphosphatase (ATPase) gene family, ATP1A1 (encoding a sodium/potassium ATPase α-subunit) and ATP2B3 (encoding a sarcoplasmic reticulum calcium ATPase) were identified by exome sequencing in these tumors. Screening for mutations in 308 aldosterone-producing adenomas found ATP1A1 or ATP2B3 mutations in 21 (7%) and KCNJ5 mutations in 118 (38%) of cases. Concomitant KCNJ5 and ATP1A1 or ATP2B3 mutations within the same tumor were never observed. Hence, mutations in *ATP1A1*, *ATP2B3*, and *KCNJ5* were found in about 50% of aldosterone-producing adenomas. Novel somatic mutations in *CACNA1D*, which encodes a L-type calcium channel, were found very recently in APAs. These findings overall suggest that, in a not negligible percentage of APAs, development of the neoplasia derives from somatic gene mutations that alter intracellular calcium homeostasis (Azizan et al, 2013; Scholl et al, 2013).

AIMS

AIMS

Somatic KCNJ5 mutations are highly prevalent in APA. Therefore, we performed a study

i). To determine the prevalence of somatic KCNJ5 mutations associated with aldosterone producing adenoma (APA) in two large Italian referral centers.

ii). To find out new mutations in KCNJ5 gene in the APA.

iii). To characterize the novel KCNJ5s-insT149 mutation detected through the screening analysis.

MATERIALS AND METHODS

MATERIALS AND METHODS

Human adrenal samples

The current study was approved by Ethics Committee. All patients gave an informed consent and the use of tissues followed our institutional guidelines. The diagnosis of Aldosterone Producing adenoma (APA) was based on the following "four corner criteria," as previously defined (Rossi et al, 2006a): 1) biochemical diagnosis of PA, 2) lateralization of aldosterone secretion at AVS, or evidence of lateralized uptake of ^{131}I-norcholesterol at dexamethasone-suppressed adrenocortical scintigraphy, 3) evidence of adrenocortical nodule at histopathology, and 4) cure or improvement of hypertension and correction of the biochemical picture of PA at follow-up after adrenalectomy.

Cure was defined as systolic blood pressure <140 mm Hg and diastolic blood pressure <90 mm Hg without medications, and improvement as systolic and diastolic blood pressure <140/90 mm Hg, respectively, on the same or a reduced number of medications and/or a reduced number of defined daily doses (WHO;, 1999). Identified APA Patients underwent laparoscopic adrenalectomy.

Tissues were obtained under sterile conditions at surgery, in the operating room and the excised adrenal gland was cut into halves according to the size of the APA. Half of the adrenal was sent to the Pathology department for histological study and the remaining tissue was divided into 2 pieces: the first was rapidly frozen in liquid nitrogen vapor state for further molecular studies, the second was processed for the isolation of CD56 positive cells.

Corresponding APA and venous blood DNAs were obtained from patients undergoing adrenalectomy for hypertension with primary aldosteronism and adrenocortical tumor at the Department of Medicine-DIMED, Internal Medicine 4 and Endocrinology units of the University of Padova and Department of Internal Medicine University "La Sapienza," Rome. All APAs were verified by histopathology and moreover all patients displayed normokalemia and improvement in blood pressure control at postoperative.

APA - DNA preparation and genotyping

Genomic DNA was prepared from subject venous blood and tumor tissue by standard procedures (Eurogold DNA Extraction kit, Euroclone, Milan, Italy). Exon 2 KCNJ5 gene was amplified using appropriate primers. PCR was performed on 250 ng DNA in a final volume of 50 µl containing 300 nM $MgCl_2$, 400 nMol each primer 200 µM deoxynucleotide triphosphate, and 2.6 U expand high-fidelity enzyme mix (Roche Applied Science, Italy). PCR product were purified using QIAquick DNA purification kit (QIAGEN,Courtaboeuf Cedex, France) and quantified with Nanodrop 2000c spectrophotometer (ThermoScientific, Wilmington, DE). Direct Sanger was performed using the ABI Prism Big Dye Terminator version 3.1 cycle sequencing kit (Applied Biosystems, CA) on an ABI Prism 3700 DNA analyzer (Applied Biosystems, CA). In the patients with mutated APA concomitance of germ-line Kir3.4 mutations was sought for by sequencing DNA from peripheral blood leucocytes or adrenal tissue surrounding the APA.

APA - cDNA preparation and genotyping

cDNA synthesis and sequencing: Mutated APA sample's total RNA was prepared from liquid nitrogen preserved APA tissue using RNAeasy kit (QIAGEN, Milan, Italy) according to the manufacturer's instructions. DNA-free RNA was prepared using DNAseI (Ambion, Life Technology, CA). Reverse transcription of 1µg RNA was performed with random hexamer primers using the Iscript cDNA Synthesis kit (Bio-Rad Laboratories, Milan, Italy) according to the manufacturer's instructions. KCNJ5 cDNA was amplified using intron-spanning primers (Table 1) and sequenced.

High resolution melting (HRM) analysis

Genomic DNA from APA corresponding peripheral blood leukocytes was amplified using SsoFast EvaGreen supermix (Bio-Rad) and primers as described (Table 1). Short amplicon covering mutation region of the KCNJ5 gene was amplified using the CFX96 real-time PCR detection system (BIORAD), and results were analyzed using the CFX Manager™ and Precision Melt Analysis™ software. The PCR reaction was performed in a 20 µl final reaction volume containing 200 nmol of each primer and SsoFast^{TM} EVA Green 5X SuperMix (Bio-Rad, USA). The system amplification protocol was 95°C for 3 min; 50 cycles of 95°C for 10 s,

60.°C for 30 s. Subsequently**,** a melt curve was generated by heating from 65°C to 95°C with 0.2°C increment. Precision Melt Analysis software was then used to identify areas of stable pre-and post-melt fluorescence from the HRM curve and automatically determined a cluster of each genotype. Some positive (SNP) and negative (wild type) controls were examined in the same PCR and melt reaction to verify the precision of melt analysis. From each cluster one samples was done Sanger sequence in order to confirm the false positive samples.

Cell culture

HAC15 cells were seeded in 6 and 12 wells plates according to the functional assay. Growth media for H295R and HAC15 cells used RPMI and DMEM-HAM-F12 respectively. RPMI Medium was supplemented with 10% fetal bovine serum (Sigma), antibiotics and 1% insulin/transferrin/selenium Premix (BD Biosciences) and of DME/F12 medium supplemented with 10% cosmic calf serum (HyClone,Logan, UT), antibiotics and 1% insulin/transferrin/selenium Premix (BD Biosciences).

RNA isolation

Total RNA was extracted from Aldosterone Producing Adenomas (APAs) and transfected HAC15 H295R, using RNeasy Mini Kit (Qiagen) following the manufacturer's protocol. Cells were collected by trypsinization and lysed in 350 µl buffer RLT with 10 µl/ml β-mercaptoethanol. Cell lysate was mixed with 70% ethanol and than transferred into column filter that selectively bound RNA. Purified RNA was eluted in 30 µl RNase-free water. On the other hand, cryoconservated adrenal tissue was mixed in 600 µl lysis buffer (594 µl buffer RPE, 6 µl β-mercaptoethanol). Tissue was omogenized with Roche Tissue Lyser, the disgregated sample was centrifuged and supernatant was mixed with 70% ethanol. Sample was transferred into column filter that selectively bound RNA. Purified RNA was eluted in 40 µl RNase-free water.

The integrity and quality of the RNA were systematically checked with the use of the lab-on-chip technology in an Agilent Bioanalyzer 2100 (RNA6000 Nano Assay, Agilent Technologies, Santa Clara, CA). The instrument uses capillary electrophoresis to analyze nucleic acid and results are visualized as electropherograms. We started from 1 µl of total RNA and, after the run, proceeded with the analysis of the resulting electropherograms. Only samples with two

distinct ribosomal peaks (18S and 28S) were used for the downstream analysis. The RNA amount and quality was evaluated with spectrophotometric readings at 260/280 and 260/230 nm.

Real-time RT-PCR analysis

One µg of total RNA was reverse transcribed with iScript ™ cDNA Synthesis Kit (Bio-Rad, Milan, Italy) in a final volume of 20 µl following the manufacturer's instructions. Samples were incubated for 5 minutes at 25°C, for 30 minutes at 42°C and for 5 minutes at 85°C and hold at 4^0C (Delphi 1000TM Thermal Cycler, Oracle, BioSystemsTM, Italy). PCR for the amplification of various target genes was then performed. Target genes Primers (Table 1) for RT-PCR were designed using Roche-applied-science Universal Probe Library site, Operon Biotechnologies and BLAST site. The reaction was performed following manufacturer's protocol in 20 µl composed of 10 µl Probes Master (Roche), primers forward and reverse 200 nM, probe 200 nM and 3 µl of cDNA sample. PCR was performed in a real-time LightCycler®480 Software (Roche, Monza, Italy), with amplification cycles of 10 s of denaturation at 95^0C, 30 s of annealing at 60^0C, and 5 s of extension at 72^0C. Total number of cycles was 35. The amplification efficiency of the target was equal to that of the internal control. PBGD was used as the endogenous reference in the comparative comparative Ct ($2^{-\Delta\Delta Ct}$) method.

Molecular cloning

Human full length KCNJ5 (#SC119590) and KCNJ3 (#SC118769) was obtained from Origene, MD, USA. KCNJ5 mutations (T158A and insT149) were inserted using the PCR based QuikChange II XL Site Directed Mutagenesis kit (Stratagene, Santa Clara, CA). After site directed mutagenesis, plasmids were transformed in DH5α E.coli and harvested plasmid's full length were sequenced in order to confirm the mutation insertion and to find out any other unspecific mutation during PCR amplification. Using appropriate primers (Table 1) KCNJ3 and KCNJ5 coding region were linked in addition to self-cleaved "2A like peptide" sequences by Gibson Assembly (Gibson Assembly® Master Mix, NEB, USA) that provides KCNJ3-2A-KCNJ5 sequence for wild type and mutations. In addition to this construct eGFP-IRES-Puro sequence was following in separate promoter region. The insertion of the

mutation is of the mutations were confirmed by a PCR-based direct sequencing method. This plasmid construct were transfected in HAC15 cells by electroporation (Nucleofector® kit, Lonza, Amaxa Inc.USA) for expressional and measurement of aldosterone studies.

For electrophysiology studies and Ca^{2+} measurement a plasmid construct was generated as follows; the mutation c.446insAAC of KCNJ5 (resulting in the mutant protein KCNJ5-insT149) was generated by site-directed mutagenesis human KCNJ3 and KCNJ5 cDNAs from Invitrogen/Geneart, Life Technologies GmbH, Germany). For expression in mammalian cells, cDNAs were subcloned into the bicistronic expression vector pIRES-CD8 (Fink et al, 1998). HEK293 cells were transfected with wild-type KCNJ5 or mutant KCNJ5-insT149 plasmids using an electroporation system (NEON, Life Technologies GmbH, Darmstadt, Germany), according to the manufacturer's protocol using 2 pulses of 20 ms at 1150 V. After electroporation, cells were cultured in antibiotic-free medium on fibronectin/collagen-coated glass cover slips. For patch-clamp or Ca^{2+} measurements, transfected cells were identified using anti-CD8 coated dynabeads (Life Technologies GmbH, Darmstadt, Germany).

Immunohistochemistry

Four µm thick serial sections from paraffin blocks of rat and human normal adrenal gland were processed for immunohistochemistry. The sections were dewaxed with 5 minutes incubations with decreasing concentration of ethanol and rehydrated with distilled water. Immunohistochemistry were performed using CYP11B2 and both CYP11B1 and CYP11B2 antibodies (1). Paraffin embedded adrenal was cut at 5 µm and the sections dried, then melted at 56°C for at least 3 h. After deparaffination through alcohols, slides were subjected to antigen retrieval using Trilogy (Cell Marque Corporation, Rocklin, CA) in autoclave, 15 min at 121°C and then treated with phenylhydrazine 0.1% for 20 min to inhibit endogenous peroxidases. Slides were blocked with Tris 0.1M, goat serum 5% or horse serum 5%, SDS 0.5%, pH 7.4 for 1 h and then incubated with CYP11B2 antibody (hCYP11B2-41-17B clone 1/500 dilution) or both CYP11B1 (CYP11B1-80-7-5 clone 1/200 dilution) and CYP11B2 (hCYP11B2-41-17B clone 1/500 dilution) overnight at 4°C. After washing, slides were incubated with secondary antibodies 1h at room temperature. We

used mouse Polink-2 Plus HRP (GBI labs, Mukilteo, WA), for CYP11B2 immunostaining; rat Polink-2 Plus AP (GBI labs, Mukilteo, WA) and ImmPRESS anti-mouse Ig reagent (VectorLaboratories, Burlingame, CA) for double immunostaining. Slides were developed using DAB and HighDef green IHC chromogen AP (Enzo Life Sciences, Farmingdale, NY). All Samples were counterstained with Meyer Hematoxylin (Vector Laboratories, Burlingame, CA) before mounting.

Immunofluorescence

Triple immunofluorescence was done using CYP11B1, CYP11B2 and 17α- Hydroxylase (2) antibodies. The protocol we followed was the same as the double immunohistochemistry. Primary antibodies incubation was done with a mixture of rat CYP11B1-80-7-5 clone 1/200, mouse CYP11B2-41-17B clone 1/500 and rabbit anti 17α-hydroxylase 1/300 overnight at 4°C. After washing, a combination of highly absorbed antibodies were used, goat anti-mouse IgG Alexa Fluor 488, goat anti-rat IgG Alexa Fluor 594 and goat anti-rabbit IgG Alexa Fluor 647 (Jackson Immunoresearch Inc. Allentown, PA) 1/1000 dilution for 1h at room temperature. The slides were then washed and mounted with Vectashield HardSet Mounting Medium with DAPI (Vector Labs, Burlingame, CA). The samples were then photographed using an Eclipse Nikon Microscope with a Rover camera and pseudocolored.

Electrophysiological characterization of the KCNJ5-insT149 mutant

Patch-clamp recordings were performed using an EPC-10 amplifier without leak subtraction (HEKA, Germany). The following solutions were used (all concentrations in mM): control solution: pH 7.4; 10 HEPES; 140 NaCl; 5 KCl; 1.8 $MgCl_2$; 1.8 $CaCl_2$, 5 glucose. Na^+-free solution: pH 7.4; 10 HEPES; 5 KCl; 1.8 $MgCl_2$; 1.8 $CaCl_2$; 140 N-methyl-D-glucamine chloride (NMDG-Cl), 5 glucose. Pipette solution: pH 7.4; 5 HEPES; 140 KCl; 4 $MgCl_2$; 1 $CaCl_2$; 1 EGTA.

Ca^{2+} measurements

Cytoplasmic Ca^{2+} was measured using adrenocortical carcinoma NCI-H295R cells transfected with wild-type KCNJ5 or mutant KCNJ5-insT149 plasmids (electroporation with NEON system using 1 pulse 40 ms at 1100 V). Before measurements, cells were loaded for 45 min with 0.5 μM of Ca^{2+}-sensitive dye Fura-2-AM in the presence of Power Load permeabilizing reagent (Molecular Probes, Darmstadt, Germany). Mean fluorescence ratios of emission at

490-530 nm after excitation at 340 nm and 380 nm were calculated for single transfected cells using Axiovision software (Zeiss, Jena, Germany) as a measure of cytosolic Ca^{2+} activity. The fluorescence ratios (340 nm/ 380 nm) were measured in transfected cells (identified by binding of anti-CD8 coated dynabeads) and non-transfected cells (without dynabeads). All the experiments were performed at room temperature.

Aldosterone measurement

HAC15 cells were transfected with 2-µg wild type and mutant KCNJ5 plasmid in 12 well plates. Prior to seed the cells plates were coated with 10 µg/ml Fibronectin (Sigma aldrich, CA). Transfection were performed using electroporation (Nucleofector® kit, Lonza, Amaxa Inc.USA). After 48 hrs of transfection cells was serum deprived in DMEM-F12 containing 0.1% cosmic calf serum for over night. After 24 hrs serum deprived in DMEM-F12 supernatants collected to assess aldosterone concentration. RNA was extracted from HAC15 cells with the RNeasy Mini kit (QIAGEN) after 24 hrs of transfection; the cell culture medium was collected for aldosterone measurement (with the Aldosterone Elisa Kit from Alpha Diagnostic International, San Antonio, TX, USA) following producer's protocol. To this end cell medium (50 µl) was added to aldosterone-coated wells and the signal was detected in an Elisa Reader (Perkin Elmer, Monza, IT). To adjust for differences of cell number across cell batches aldosterone levels were normalized to the amount of cell RNA content.

Molecular modeling of the KCNJ5-insT149 mutant

A model of the KCNJ5 tetramer, amino acids from 51 to 370, was built by homology modeling with the webserver Swiss-Model (Arnold et al, 2006) using as a template the crystal structure of the inward rectifier K^+ channel Kir3.2 (PDB code 3SYA). The latter presents 85% sequence identity with our protein. A threonine was inserted at position 149 with the graphic program Coot, (Emsley & Cowtan, 2004) and the model adjusted by hand and optimized by molecular dynamics with software CNS. (Brunger, 2007) 30,000 steps of dynamics at room temperature were performed. All atoms were harmonically restrained during the dynamics, with the exception of residues from 129 to 160, that include the selectivity filter of the channel, that were left free to move. A restrain to maintain the four-

fold symmetry of the tetramer was applied to all atoms of each monomer during the simulation process.

Statistical analysis

Results were expressed as mean ± SE of at least 3 separate experiments in which each samples was assayed in triplicate or quadruplicate. Differences between groups were analyzed by t-test and, for multiple groups' comparison, by one-way ANOVA followed by Bonferroni comparisons. The differences were considered to be significant at $P < 0.05$. Statistical analyses were performed using Graphpad/prism 5 for Windows software (GraphPad Software, La Jolla, California, USA; www.graphpad.com).

TABLE 1: Primer sequences

Gene	Accession Number	Primer	Sequence
KCNJ5	NM_000890.3	For-Seq	5’-cctcaagtggcgcttcaact-3’
		Rev-Seq	5’-ctttggtctgccgggactt-3’
		For-HRM	5’-cgaccaagagtggattcctt-3’
		Rev-HRM	5’-agggtctccgctctcttctt-3’
		SDM1-T158A	5’-cttccgagtcatcgcagagaagtgtcc-3’
		SDM2-T158A	5’-ggacacttctctgcgatgactcggaag-3’
		SDM1-insT149	5’-ttctccattgagaccgaaacaacaaccatt gggtatggcttccgagtc-3’
		SDM1-insT149	5’-gactcggaagccatacccaatggttgttg tttcggtctcaatggagaa-3’
		Gib-Ass-1	5’-gagggcagaggaagtctgctaacatgcggtgacgtcg aggagaatcctggcccaATGGCTGGCGATTCTAGG-3’
		Gib-2A Vec1	5’-TGCCGTGGTGCACATT-3’
		Gib-Ass-2	5’-tgggccaggattctcctcgacgtcaccgcatgttagcag acttcctctgccctc TGTGAAGCGATCAGAGTTCATTT-3’
		Gib-2A-Vec2	5’-acaggggcagatcaacttttt-3’
		For-qPCR	5'-ggaagctccgatctcaacaa-3'
		Rev-qPCR	5'-cctggttcatggcattccta-3'
CYP11B1	NM_001026213.1	For-qPCR	5’-ccatctttatgtcctcttgggtta -3’
		Rev-qPCR	5’-cctggcagaggcagagat -3’
CYP11B2	NM_000498.3	For-qPCR	5’- gagcagggttatgagcac-3’
		Rev-qPCR	5’- gtggtcctcccaagttgta-3’
PBGD	NM_000190.3	For-qPCR	5’-tgccctggagaagaatgaag -3’
		Rev-qPCR	5’-agatggctccgatggtga -3’

RESULTS

RESULTS

KCNJ5 mutation status

DNA sequencing from 195 consecutive APA patients, who were enrolled in two Italian referral centers and underwent adrenalectomy, showed a prevalence of KCNJ5 somatic mutations of 24.1%. Of these, 27 (11%) , 17 (7%), and 3 (1.2%) exhibited G151R, L168A and T158A mutations, respectively (Figure 1). The prevalence of such mutations differed between the centers, being 29.3% and 12.7%, respectively in Padua and Rome.

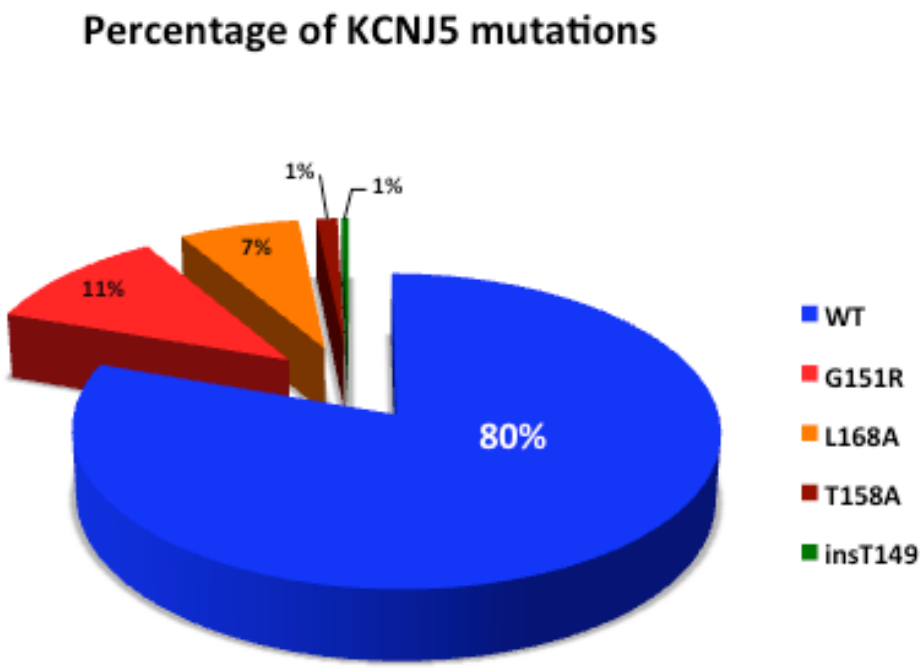

Figure 1. Percentage of KCNJ5 mutations in APA patients from three different Italian populations: KCNJ5-WT, G151R, L168A, T158A and novel InsT149 mutations depicted.

A novel c.446insAAC insertion was found in a patient with severe drug-resistant hypertension. This insertion was absent in the corresponding peripheral blood DNA and adjacent adrenal gland tissue, thereby demonstrating its somatic nature. Moreover, we found that c.446insAAC insertion resulted in the mutant protein KCNJ5-insT149.

When considering also the novel insertion mutation, percentage of mutated APAs raised from 24.1%. to 24.49% (Table 2).

Table 2. Type and Frequency of KCNJ5 Mutations in APA in two Italian centers

Centers	APAs (No)	G151R	L168A	T158A	ins T149	Prevelence (%)
Padova	140	25	12	3	1	29.3
Rome	55	2	5	0	0	12.7
Total	**195**	**27**	**17**	**3**	**1**	**24.6**

Total mutations found in 195 APA patients comprised G151R (56.3%), L168A (35.4%) and T158A (6.3%).

Gender differences and KCNJ5 mutations

KCNJ5 in and near selectivity filter mutations studies showed clear gender dimorphism. Our APA population confirmed a difference in the prevalence of KCNJ5 mutations between women and men (Figure 2). Male and female ratio among APA patients was in equal proportion (Figure 2B), with KCNJ5 mutations in 75% APAs in women and in 25% APAs in males (Figure 2A).

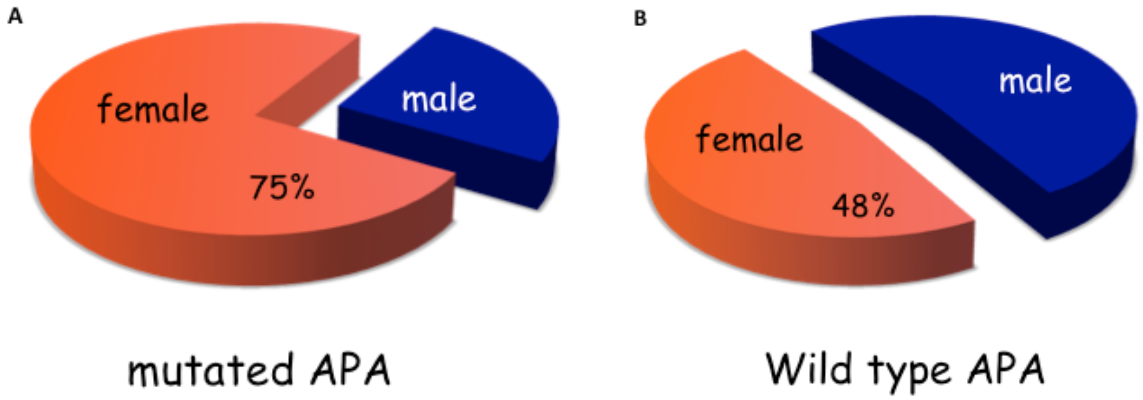

Figure 2. Gender differences between the KCNJ5 mutated and wild type APA patients:

KCNJ5 mutations are more recurrent in lesions from female patients, representing a distinct gender dimorphism. Gender differences significance analyzed by $p<0.01$ by Fisher's Test.

TABLE 3. Clinical features at baseline and follow-up of the APA patients divided according to the presence or absence of KCNJ5 mutations

	Wild type APA (n=62)			Mutated APA (n=29)		
Variable	Baseline	Follow-up	p	Baseline	Follow-up	p
Systolic BP (mmHg)	161 ± 2	130 ± 2	0.001	159 ± 2	131 ± 2	0.001
Diastolic BP (mmHg)	99 ± 2	82 ± 1	0.001	97 ± 2	84 ± 1	0.001
Serum K^+ (mmol/L)	3.2 ± 0.1	4.2 ± 0.1	0.001	3.1 ± 0.1	4.1 ± 0.1	0.001
PRA (ng/mL /h)	0.47 (0.20-0.66)	1.85 (1.10-2.77)	0.001	**0.24 (0.20-0.43)***	2.00 (1.47-2.46)	0.001
PAC (ng/dL)	37.2 (20.4-59.8)	15.0 (9.70-15.0)	0.001	**54.8 (30.7-80.7)****	15.0 (9.2-15.0)	0.001
ARR (ng/dL):(ng/mL /h)	75.0 (43.5-155.0)	11.45 (8.07-15.53)	0.001	**157.3 (76.8-372.9)*****	9.6 (6.2-18.0)	0.001
Medication score	**2.1 ± 0.2**	**1.1 ± 0.1**	**0.001**	**1.9 ± 0.2**	**0.6 ±0.1***	**0.001**

** p < 0.05; ** p < 0.03; *** p < 0.01 mutated APA *vs* wtAPA

Clinical features at baseline and follow-up of the 91 APA patients divided according to the presence (29) or absence (62) of KCNJ5 mutations (Table 3). The APA patients did not differ

significantly from the whole population for demographic and biochemical variables; therefore, they considered to be representative of the whole population. All patients showed a high aldosterone to renin ratio (ARR) at baseline. After adrenalectomy they exhibited a fall of BP despite a reduction of the number of antihypertensive drugs along with normalization of serum K^+ and ARR ($P < 0.001$;Table 3)

KCNJ5 mutations screening by high melting resolution (HRM)

Peripheral blood or adjacent adrenal gland from the same patients investigated for the APAs were used to search for genomic/familial variation(s) in mutated APA samples. By using HRM after real-time PCR, mutated were discriminated from wild type APAs according to the different melting temperature of the corresponding amplicons. False positive samples were sequenced in order to confirm the mutations.

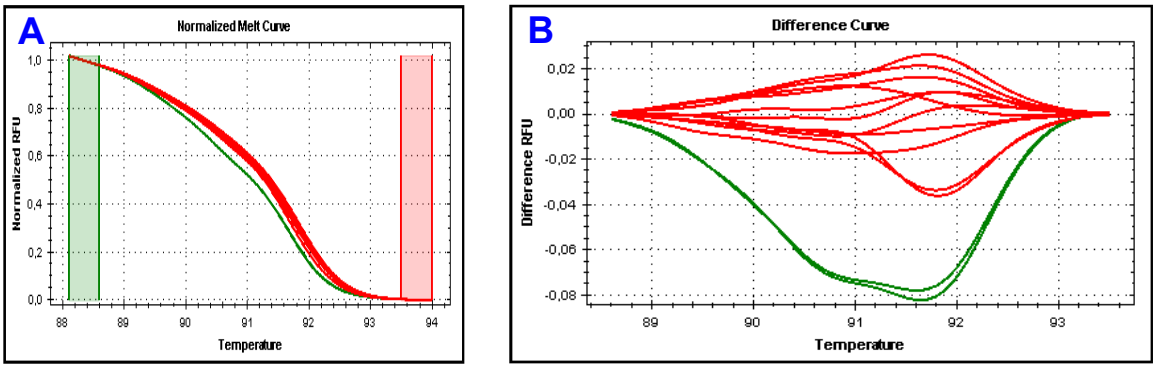

Figure 3: Normalized (A) and differential (B) graphs of the melting curves obtained from HRMA of APA samples and corresponding blood samples or adjacent adrenal gland tissue. Mutated APA samples were used as positive control. In panel A and B shows mutated in green and wild type in red.

Sequencing chromatograms of KCNJ5

Sanger sequencing traces depict KCNJ5 mutations found in our investigated APA (Figure 4), including G151R, L168A and T158A. Of interest, we found not only mutations previously shown in APAs (G151R and L168A), but also T158A, which were reported to be only in BAH.

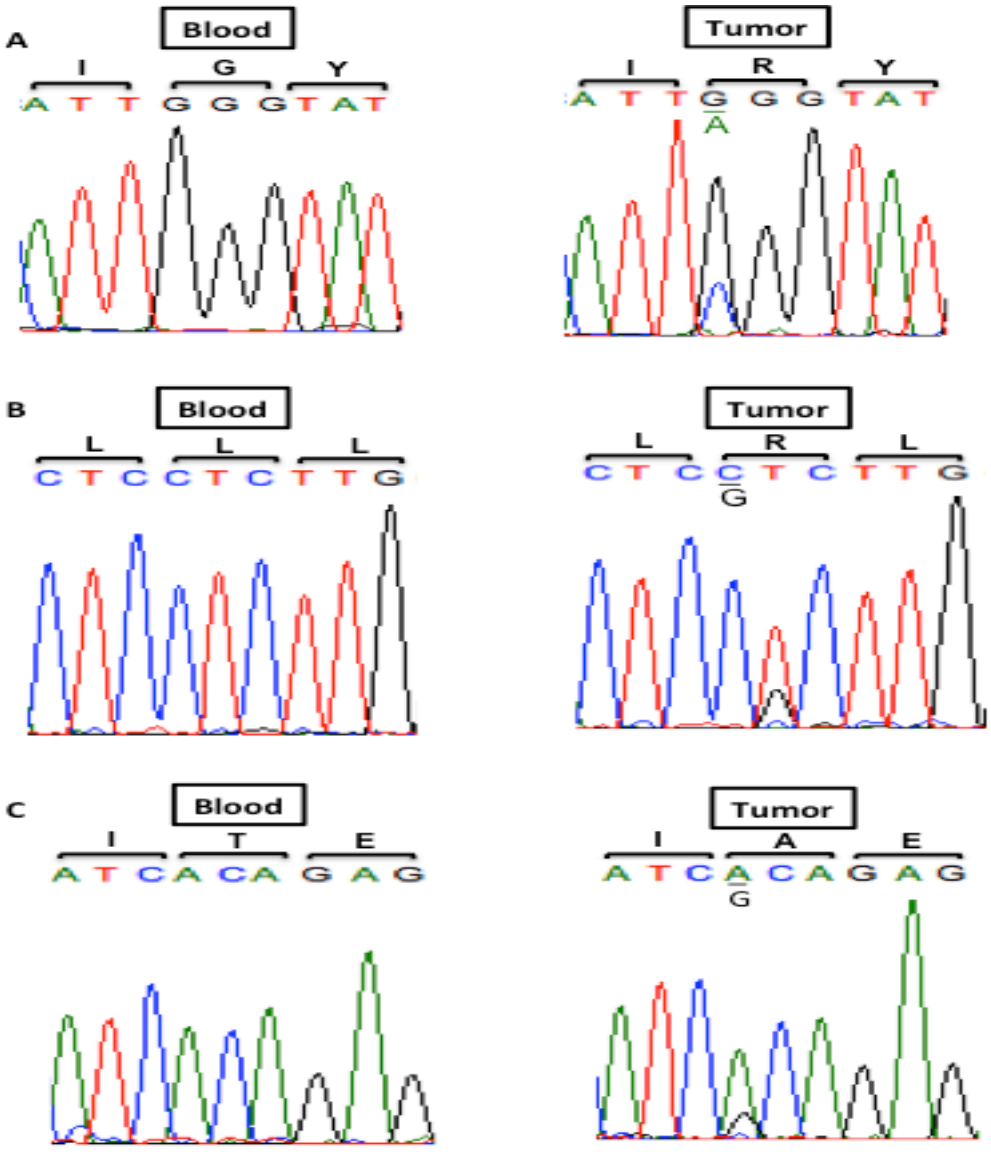

Figure 4. Sequencing chromatograms: KCNJ5 mutated aldosterone-producing adenomas (APA) or blood. Peripheral blood leukocytes or adjacent adrenal gland gDNA used to confirm the somatic status of mutations detected. A) KCNJ5-G151R B) KCNJ5-L168A and C) KCNJ5-T158A.

Clinical Case of the novel KCNJ5-insT149

The patient was 65 year-old man referred for drug-resistant hypertension. He had been hypertensive for 11 years and suffered from a stroke in 2000. On presentation his blood pressure was 183/102 mmHg supine and 170/101 mmHg standing, in spite of full adherence to treatment with canrenone 50 mg/d, telmisartan 80 mg/d, nebivolol 10 mg/d; doxazosin 2 mg/d; amlodipine 10 mg/d. His serum K^+ was 2.5 mEq/L; renin was suppressed (direct renin 3.0 µU/ml supine; 2.3 µU/ml standing and his plasma aldosterone concentration was 37.4 ng/dL supine and 61.5 ng/dL standing (n.v. < 15 ng/dl and < 10 ng/dl, respectively. He was found to have concentric left ventricular hypertrophy at echocardiographic (left ventricular mass index 171 g/m^2 ; relative wall thickness of 0.56; n.v. < 115 g/m^2 and < 0.45, respectively). On CT a 9 mm (maximum diameter) node was seen in his right adrenal gland. Hormonal retesting after adequate wash-out from interfering drugs(Rossi et al, 2011), while he was only on doxazosin 4 mg/d and slow-release verapamil 180 mg/d, showed a plasma renin activity of 0.20 ng/mL/h, both baseline and post-captopril, and plasma aldosterone concentration of 36.4 ng/dl and 31.3 ng/dl post-captopril, respectively. Hence the ARR was markedly elevated (182 baseline; 156 after captopril (n.v. <26 and <13, respectively). He therefore underwent AVS that showed a right LI of 3.49 indicating right lateralization. At laparoscopic right adrenalectomy a small adenoma was found. One month after adrenalectomy left ventricular mass index was 164 g/m^2 and a relative wall thickness of 0.58. After 2 years follow-up his ARR is 5, serum K^+ is 4.3 mEq/L, and at 24-hrs ambulatory blood pressure monitoring his blood pressure is 132/70 mmHg while on amlodipine 5 mg/d and nebivolol 5 mg b.i.d..

Thus, concomitance of long-term cure of the hyperaldosteronism and the prominent decrease of his blood pressure that became responsive to treatment, alongside AVS and pathology data, in retrospective allowed a conclusive diagnosis of APA by the four corners criteria (Rossi et al, 2006a).

Novel KCNJ5 mutation in APA

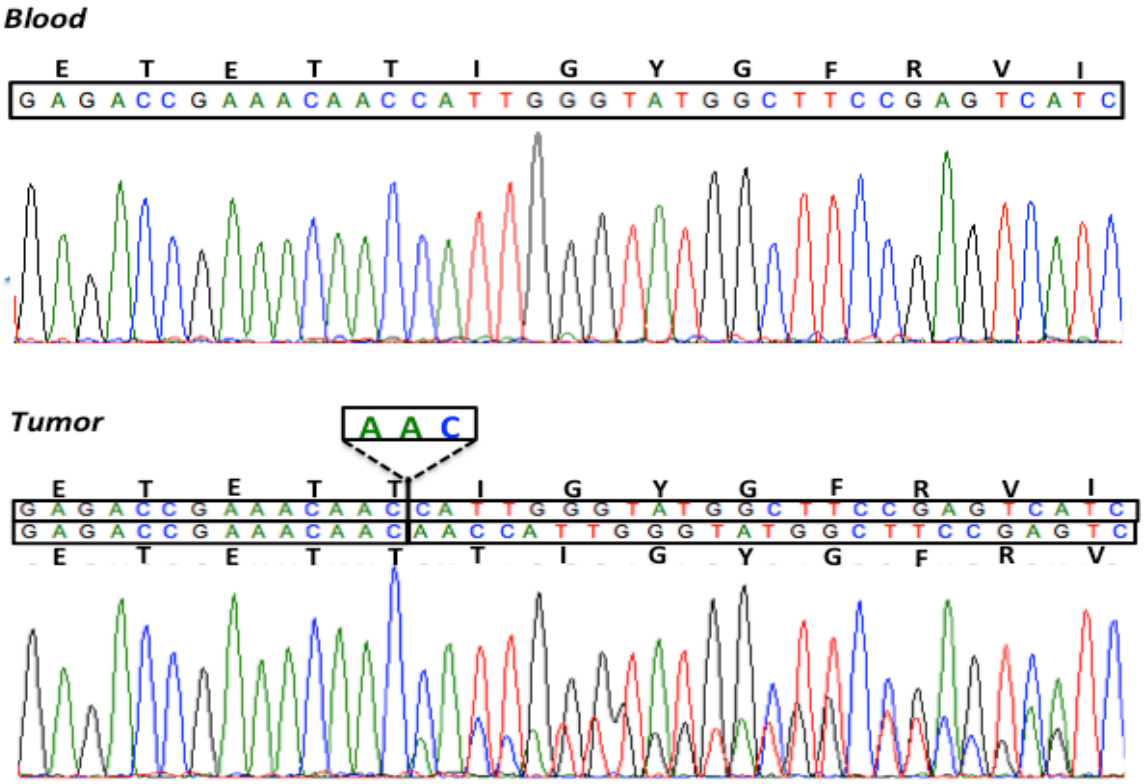

Figure 5. Sanger sequence traces: shows an in-frame 3 bp insertion at c.446 position resulting in a novel KCNJ5-insT149 mutation in a patient with drug-resistant hypertension caused by an APA.

KCNJ5 gene was amplified and sequenced from APA patient with severe drug-resistant hypertension. In APA, a novel c.446insAAC insertion mutation was found that resulted in the mutant protein KCNJ5-insT149 position (Figure 5). The insT149 mutation was identified also in cDNA by sequencing. No mutation was found in corresponding peripheral blood or adjacent adrenal tissue, thereby ensuing somatic mutation. This mutation is novel since we could not detect it in the available cancer SNPs databases.

Molecular modeling of the KCNJ5-insT149 mutation

In order to analyze the molecular impact of the novel KCNJ5-insT149 mutation we performed in-silico model using PyMOL software. Since crystal structure model for KCNJ5 protein is not available, the crystal structure of KCNJ12 channel (PDB code 3SYA), which is

similar to KCNJ5 in amino acid sequence, was considered for this analysis. The model of the KCNJ5 tetramer, amino acids from 51 to 370, built by homology modeling of this altogether novel mutation, showed that the inserted threonine 149 residue is located after the pore α-helix that precedes the selectivity filter of the K^+ channel (Figure A and B). This insertion places the threonine residue at the beginning of the filter sequence, altering its geometry, the channel selectivity and eventually producing non-selective channels, in keeping with results found with mutations at the selectivity filter or in close proximity to it .

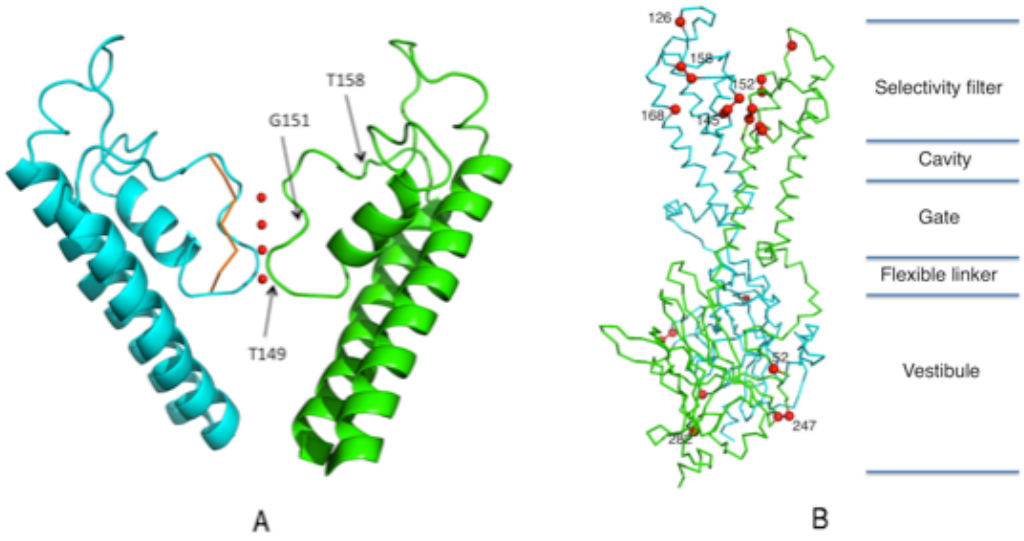

Figure 6. Cartoon drawing of the region of the selectivity region of KCNJ5-insT149 mutant after molecular dynamics model optimization: Only two chains of the tetramer, cyan and green, are shown for clarity purposes. The position of the Cα's of the selectivity filter residues in the original crystal structure is shown in orange. Small red spheres represent K^+ ions as present in the crystal structure of the KCNJ12 channel (PDB code 3SYA). The position of the inserted threonine along with that of two mutations previously found (Choi et al, 2011), is indicated by arrows. A). All the mutations found thus far in the APA's KCNJ5 gene (Figure 6 B). B). Novel KCNJ5-insT149 mutation location (Figure 6 A).

The K^+ path through the filter is guided by a line of three main chain carbonyl oxygen atoms facing the channel pore, plus the –OH group of a threonine. The insertion of a residue at one end of the pore displaces two of these carbonyls, producing a widening of the pore space. At the same time, the –OH group of the side chain a second threonine protrudes in the channel pore. The combined effect of these events are probably enough to destroy the selectivity of the filter.

Location of the novel mutations in the selectivity filter of KCNJ5 adjacent to the GYG conserved regions. Furthermore, Positions of the insT149 phylogenetically conserved region between other potassium channel and other species.

Immunohistochemistry and Double immunofluorescence

This patient had a small adrenal adenoma that stained strongly and in a fairly uniform pattern with the CYP11B2 antibody (Figure 7 A). There was an area of strong staining distant from the adenoma, one section of which has scattered cells and the other larger had relatively compact staining (Figure 7 B and C). Double staining showed that the CYP11B1 (green) was surrounding the adenoma and there were a few cells expressing the CYP11B1 within the adenoma (Figure 7 D, E and F). Triple immunofluorescence showed that the CYP11B1 and the CYP11B2 did not co-localized within the same cells, but there were CYP11B1 cells in between cells expressing the CYP11B2 enzyme (Figure 7 G). The CYP11B2 did not co-localized with the 17a-hydroxylase, but the CYP11B1 co-localized with the 17a-hydroxylase (Figure 7 H and I).

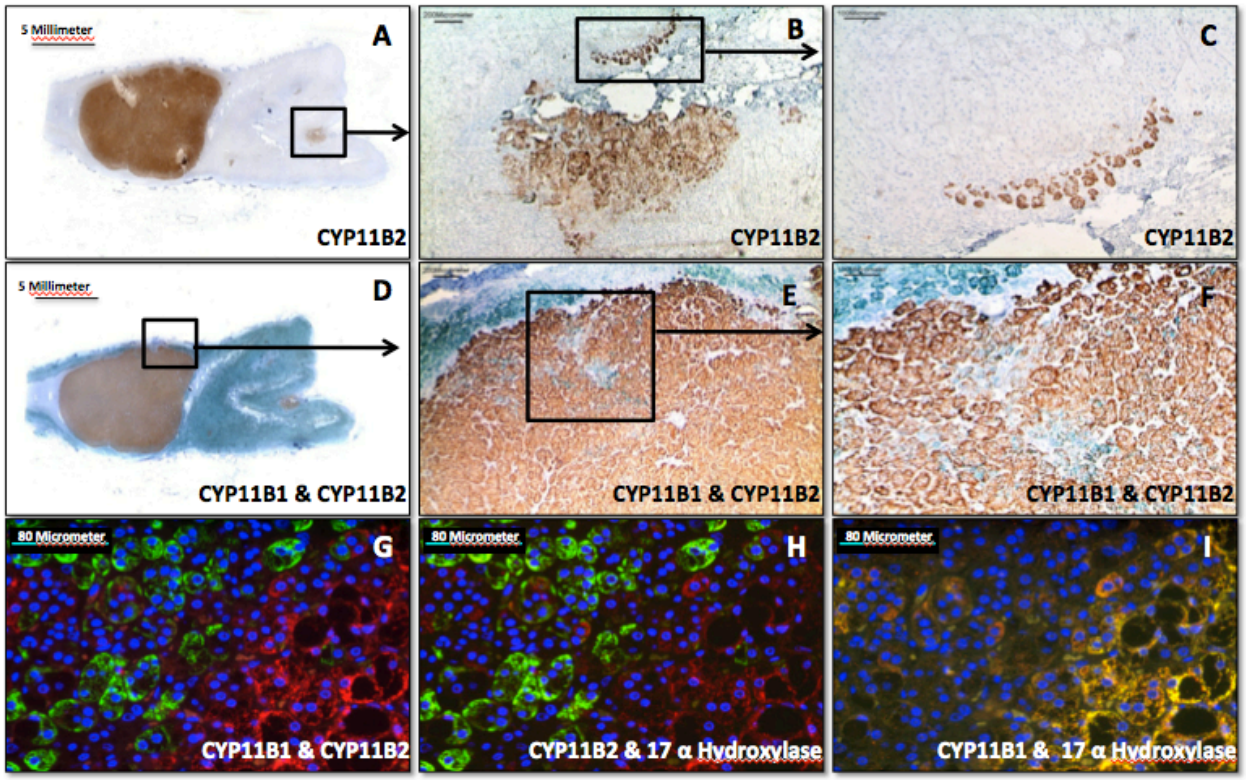

Figure 7. CYP11B1 and CYP11B2 adrenal immunohistochemistry and triple immunofluorescence for CYP11B1, CYP11B2 and 17α-hydroxylase: Panel A, B and C are different areas at higher magnification of the same adrenal stained with the hCYP11B2-41-17B antibody. Panel D, E and F are double staining for CYP11B1-80-7-5 (green) and CYP11B2 (brown) antibodies. Panel G, H and I are images of triple immunofluorescence for CYP11B1, CYP11B2 and 17α-hydroxylase at the same magnification (10X). Panel G, H and I are the merged image of CYP11B2 (green) and CYP11B1 (red) staining; CYP11B2 (green) and 17 α Hydroxylase (red); CYP11B1 (green) and 17 α Hydroxylase (red) respectively.

Electrophysiological characterization of the KCNJ5-insT149 mutant

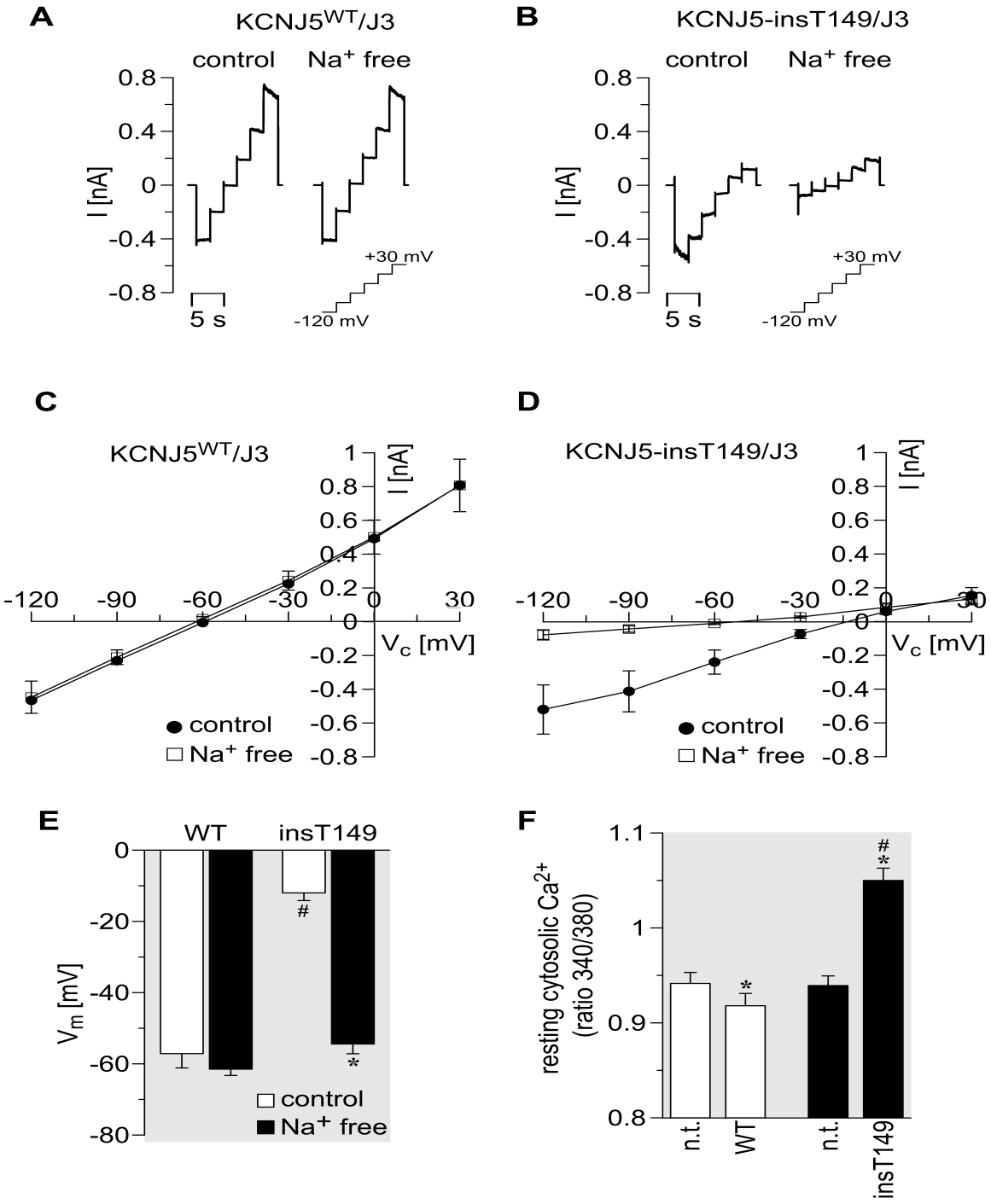

Figure 8. Basic characteristics of the KCNJ5-insT149 mutant channel in HEK293 cells (A-E), and influence of the mutated KCNJ5 on the Ca^{2+} homeostasis in adrenocortical carcinoma NCI-H295R cells (F). (A) Typical original whole cell current traces of a wild-type KCNJ5/KCNJ3

(KCNJ5WT/J3) and (B) of a mutant KCNJ5-149insAAC/KCNJ3 (KCNJ5-insT149/J3) expressing HEK293 cell are shown. Current traces were recorded in the presence of extracellular Na^+ (control) and after replacement of extracellular Na^+ by $NMDG^+$ (Na^+ free). (C, D) Summary of I/V curves of similar whole cell experiments as shown in (A,B); KCNJ5WT/J3, n=8; KCNJ5insT149/J3, n=7. (E) Effect of Na^+ replacement on the membrane voltage. *p<0.05 control vs. Na^+ free, # p<0.05 KCNJ5WT (n=8) vs. KCNJ5insT149 (n=7). (F) Ca^{2+} activity of NCI-H295R cells, as measured by Fura-2-ratios, were higher in KCNJ5insT149 cells (9 transfected cells and 13 non-transfected (n.t.) cells from 4 independent dishes), compared to wild-type KCNJ5 expressing cells (7 transfected cells and 10 non-transfected (n.t.) cells from 4 independent dishes). *p<0.05 non-transfected vs. KCNJ5WT or KCNJ5insT149 transfected cells, # p<0.05 KCNJ5WT vs. KCNJ5insT149. Values are mean values ± SEM.

In whole cell patch-clamp experiments, wild-type KCNJ5/KCNJ3 transfected cells showed inward (negative) and strong outward (positive) currents depending on the voltage-clamped. The outward currents mainly reflected K^+ efflux through K^+ channels. Whole cell currents of these cells were not changed by replacing bath Na^+ with the larger cation $NMDG^+$ (Na^+ free, Figure 4A and C). In cells expressing mutant KCNJ5T-ins149/KCNJ3 channels, the inward currents were larger and the outward currents were blunted. Replacement of extracellular Na^+ by $NMDG^+$ almost abolished the inward currents indicating that they were caused by a pathological Na^+ influx through mutated KCNJ5 channels (Figure 8 B and D). The pathological Na^+ influx led to a depolarization of the membrane voltage of cells transfected with the mutant KCNJ5-insT149/KCNJ3 compared to cells transfected with the wild-type channels (Figure 8 E). Removal of bath Na^+ led to a strong hyperpolarization of cells transfected with the mutant channels.

Ca^{2+} measurements of KCNJ5-insT149 mutations in HEK293 cells

Cytoplasmic Ca^{2+} was measured using adrenocortical carcinoma NCI-H295R cells transfected with wild-type KCNJ5 or mutant KCNJ5-insT149. As in aldosterone-producing adrenal cells, KCNJ5-insT149 mutations leads membrane depolarization that causes the opening of voltage-gated Ca^{2+} channels and a rise of intracellular Ca^{2+} that is key for the stimulation of aldosterone synthesis, we examined the effect of the adenoma-associated KCNJ5-insT149

mutant on cytosolic Ca^{2+} activity in adrenocortical carcinoma NCI-H295R cells. Cytosolic Ca^{2+} activity, as measured by the Fura-2 ratio (340nm/380 nm), was increased in mutant KCNJ5 expressing cells compared to cells with wild-type KCNJ5 (Figure 8 F). Compared to non-transfected cells of the same dishes ("n.t." in Figure 8 D), resting cytosolic Ca^{2+} was slightly decreased in cells expressing wild-type KCNJ5 (Figure 8 F) suggesting that wild-type KCNJ5 hyperpolarizes the membrane and reduces Ca^{2+} influx across the plasma membrane.

Effects of KCNJ5 mutations on CYP11B1 and CYP11B2 gene expression in mutated and non-mutated APA samples

The patients with an APA carrying the KCNJ5 mutations showed a higher prevalence of women (75% vs. 48%, P < 0.01), whereas they did not differ for age or APA size compared with those without such mutations. The amount of mRNA of *CYP11B1* and *CYP11B2* was measured in 18 APAs with the KCNJ5 mutations and 14 without them. Although the gene transcript amount of CYP11B1 did not differ between groups, that of CYP11B2 was higher (*P* = 0.015) in mutated APAs than in wild-type APAs (Figure 9).

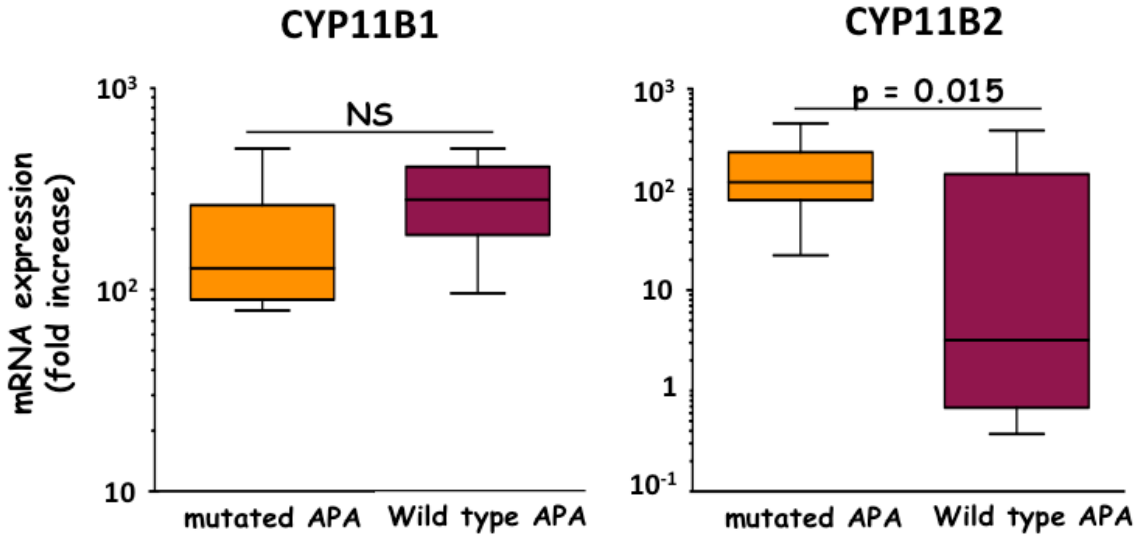

Figure 9. The box and whisker plots show gene expression of CYP11B1 and CYP11B2 in mutated and wild-type APAs, calculated as the relative ratio to the cycle threshold (Ct) levels of the housekeeping gene porphobilinogen deaminase (*PBGD*). Notably the

expression of CYP11B2 was higher in mutated than in wild-type APAs, whereas the expression of CYP11B1 did not differ.

CYP11B1 and CYP11B2 expression and aldosterone production from novel KCNJ5-insT149 transfected cells.

HAC15 cells transfected with KCNJ5 wildtype or mutated plasmid construct. Seventy-two hours after transfection with expression constructs for wild type and mutatedKCNJ5 (insT149 and T158A) together with KCNJ3. The expression of CYP11B2 mRNA in KCNJ5-insT149 cells was significantly elevated by 2-fold in comparison to control cells and wild type KCNJ5 transfected cells. However, CYP11B1 expression did not differ between wild type and mutatant transfected cells.

Since we found up-regulation of mRNA expression in mutant transfected cells, we measured aldosterone production, and found two-fold increase in KCNJ5-insT149 transfected cells compared to wild type and mock. These results suggested that over-production of aldosterone and aldosterone synthase (CYP11B2) may be related to the novel KCNJ5 mutation in APA. (Figure 10 A-C)

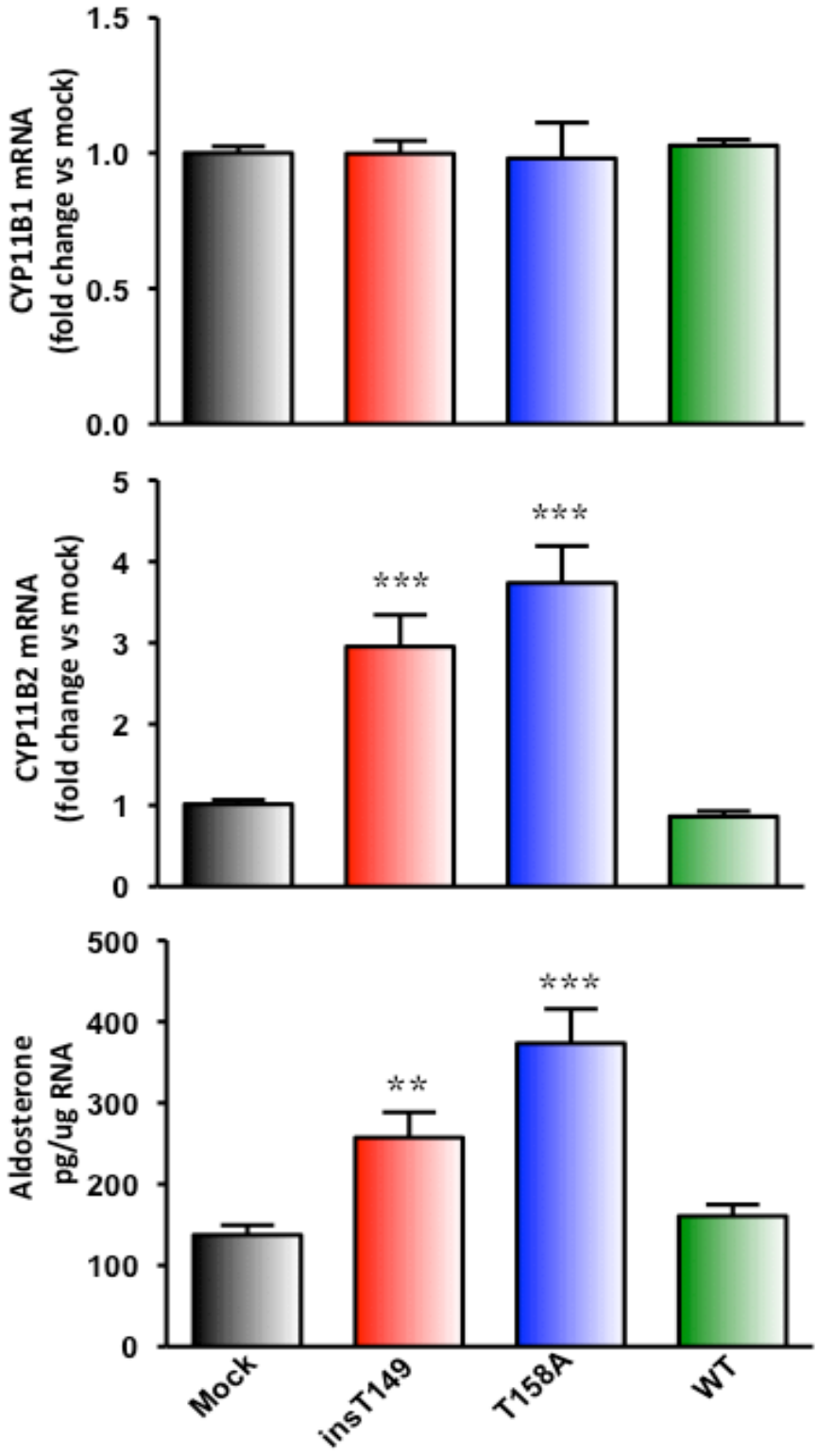

Figure 10. Effect of KCNJ5-insT149 mutation on CYP11B2, CYP11B1 expression and aldosterone production: HAC15 cells transiently transfected with either the control (Mock

transfected) or one of the mutant KCNJ5. (A). CYP11B1 mRNA expression, (B). CYP11B2 mRNA expression, and (C). Aldosterone release. Results were shown Mean ± SEM, n=6, *** P<0.001 and ** P<0.01 versus mock and wild type.

DISCUSSION

DISCUSSION

The PAPY Study provided conclusive evidence that PA is much more common than previously thought, as it involves more than 11% of the hypertensive patients referred to the specialized center (Rossi et al, 2006a). APA is the most prevalent for of PA, entailing 62.5%. The recent identification of somatic KCNJ5 mutations in APA patients could represent a breakthrough in understanding of the pathophysiologic mechanisms underlying PA. Depending on the studies, about 25% - 60% of APA has somatic mutations in the selectivity filter of the G protein-activated inward rectifying potassium channel Kir3.4 coded by the KCNJ5 gene. In our APA cohort the prevalence of KCNJ5 mutations was 24.6%. (Table 2) These KCNJ5 mutations were associated with tumor size, left ventricular mass, lateralization index, and gender dimorphism.

The selectivity filter is a conserved region within this family of channels that allows the selective transport of K^+ over other cations. Under normal physiological conditions, an increased number of Kir3.1/Kir3.4 in the membrane enhances K^+ currents and inhibits aldosterone release by activating Kir3.4/Kir3.1 in adrenal ZG cells (Choi et al, 2011). KCNJ5 mutations in the selectivity filter were found to abolish the membrane selectivity and allow other ions enter into the cells thereby leading to membrane depolarization, increased intracellular calcium, aldosterone production and CYP11B2 expression.

All mutations in the KCNJ5 channel reported thus far in APA patients, either somatic or germinal, entailed a substitution of amino acid residues in the selectivity filter (Figure 6 B), and caused enhanced aldosterone secretion (Gomez-Sanchez & Oki, 2013). G151R and L168A somatic mutations were highly prevalent in APA, and were found to reduce channel selectivity.

A screening for germline KCNJ5 mutations in familial forms of PA revealed a third heterozygous T158A mutation associated with bilateral adrenal hyperplasia. However recent reports suggested that T158A can also occur in APA and, therefore, it may be somatic. Other mutations in or surrounding the selectivity filter have been found, including R52H, E145Q, E145K, G151E, Y152C, I157C, delI157, T158A, E246K, G247R and E282Q.

Overall in our two cohorts we could identify only somatic mutations including three KCNJ5 mutations (G151R, L168R and T158A) that were previously reported. Their rates are shown In Figure 1. In addition we identified an altogether novel KCNJ5 insT149 somatic mutation (Figure 5) in a patient presenting with severe (Stage III) drug-resistant hypertension..

These mutated patients showed higher plasma aldosterone levels than the wild-type APA patients (TABLE 3), because of a higher secretion of aldosterone from the APA. This explains why the lateralization index was significantly higher than in those without such mutations. Similarly, the secretion of aldosterone in the contralateral adrenal gland was suppressed far more commonly in the mutated APA than in the wild type APA, likely because of the higher production of aldosterone in the mutated tumors. In fact, we found a higher CYP11B2 mRNA in the mutated than in the mutated APA than in the wild type APA (Figure 9).

Novel KCNJ5-insT149 mutation

The novel KCNJ5-insT149 mutation consists of insertion of a threonine residue at the end of the pore α-helix that precedes the selectivity filter of the K^+ channel (Figure 6 A and B). This mutation is unique in that it implied the addition of one threonine 149 residue in the area and could significantly alter the geometry of the filter and the control of its selectivity for cations despite not being in the filter as mutations at the filter or in close proximity to it were found to alter the channel selectivity and eventually produce non-selective channels.

To challenge the hypothesis that novel insT149 mutations could affect aldosterone production, the human adrenocortical HAC15 cells were transfected with the mutant KCNJ5-insT149 together with KCNJ3, a subunit that assembles with KCNJ5 to form native channels, showed an increased aldosterone production and expression of the CYP11B2, but not the CYP11B1 gene, compared to mock-transfected cells and to cells transfected with the wild-type channel (Figure 10 A - C).

To further characterize the functional consequences of this novel mutation we performed whole cell patch-clamp experiments in HEK293 cells transiently transfected with mutant or wild-type KCNJ5, and KCNJ3. We found that wild-type KCNJ5/KCNJ3 transfected cells

showed inward (negative) and strong outward (positive) currents, mainly reflecting K^+ efflux through K^+ channels, depending on the voltage-clamp. Replacement of Na^+ with the larger cation $NMDG^+$ (Na^+ free, Figure 8 A and C) did not change whole cell currents of these cells. By contrast, in cells expressing mutant KCNJ5-insT149/KCNJ3 channels, the inward currents were larger and the outward currents were strongly decreased.

Replacement of extracellular Na^+ by $NMDG^+$ almost abolished the inward currents, thus indicating that these inward currents were caused by a pathological Na^+ influx through mutated KCNJ5 channels (Figure 8 B and D). The abnormal Na^+ influx led to a depolarization of the membrane voltage of cells transfected with the mutant KCNJ5-insT149/KCNJ3 compared to cells transfected with the wild-type channels (Figure 8 E). Removal of bath Na^+ led to a strong hyperpolarization of cells transfected with the mutant channels. Of note, cells transfected with the mutant channels showed a prominent highly significant increase of cytosolic resting Ca^{2+} as compared to either non-transfected, or to cells transfected with the wild-type construct (Figure 8 F).

Taken together, these results indicate that the KCNJ5-insT149mutation, similar to other APA-associated KCNJ5 mutations, conferred a pathological Na^+ permeability to the channel resulting in cell depolarization, and activation of Ca^{2+} influx. The latter promoted stimulation of aldosterone synthesis and possibly adenoma formation.

Fourteen other mutated (or deleted) positions were previously found in PA patients: 10 in the selectivity filter and 4 away from it (Figure 6 B). Of them, only two (151 and 152) involve residues directly overlooking the selectivity filter: residue 151 is a glycine and both mutations (G151R and G151E) introduce a cumbersome charged side chain in an already crowded area, thus strongly perturbing the filter from the standpoint of both size and charge. Accordingly, both mutations were functionally described to alter ion conductivity and depolarize the membrane.

Mutation Y152C has an opposite conformational effect, because a bulky side-chain that points in the opposite direction with respect to the ion channel is substituted by a smaller one. The -OH group of tyrosine 152 forms a H-bond interaction with threonine 146; the loss

of the interaction, coupled to the vacuum generated by the substitution destabilizes the selectivity filter, as demonstrated by the functional effects on ion conductance.

Five mutated positions (126, 145, 157, 158, and 168) localize in the selectivity filter domain, but not directly in contact with the ion tunnel. The most marked effect was observed for L168R: the introduction of a positively charged side chain in a mostly hydrophobic environment strongly perturbs the 3-dimensional structure, and these effects likely influence the channel conductance. The conformational effects of the T158A substitution are less evident, but the presence of an H-bond between the –OH group of threonine and the carbonyl oxygen of proline 128 in the native structure suggests some destabilization of the structure and of the overall domain. The relevance of this portion of the selectivity filter region is also supported by the deletion of position 157 or its mutation from isoleucine to serine, which has also significant functional effects on conductivity. Substitution E145Q, despite being conservative with respect to the size of the side chain, destroys the potential salt bridge between glutamic acid 145 and arginine 155. Finally, tryptophan 126 is located on a loop of the selectively filter region fully exposed to the solvent, and the only consequence of its mutation to an arginine is a modification of the electrostatic potential of the local surface.

The remaining four mutated positions (52, 246, 247, and 282) are located in the vestibule domain of the KCNJ5 channel (Figure 6 B), which has been proposed to be a key component of the gating mechanism (Kuo et al, 2003). The mutations have been found to increase Na^+ conductance and to loose K^+ selectivity. Mutations E246K, G247R and E282Q involve residues located on the surface of the vestibule domain, and they can be easily accommodated with minor local rearrangements, the only consequence being a modification of the local electrostatic potential. The effects of mutation R52H are trickier, since arginine 52 located at the N-terminus of the protein forms a salt bridge with glutamic acid 326 and H-bonds with carbonyl oxygen of serine 321 and methionine 54. In this way it helps to stick the N-terminus of the protein to the C-terminal vestibule domain. Substitution of this residue with a histidine weakens this interaction, with unpredictable conformational effects on the K^+ transport process.

CONCLUSIONS AND PERSPECTIVES

CONCLUSIONS AND PERSPECTIVES

This study in a relatively large cohort of patients with an unequivocal diagnosis of APA confirms that somatic mutations of the Kir3.4 channel are common, while germline mutations are probably exceedingly rare. We also showed that there is a higher expression of the aldosterone synthase (CYP11B2) gene in aldosterone-producing adenomas with the KCNJ5 mutations than in those without such mutations.

Furthermore, this work provided the following novel pieces of evidence: a novel threonine insertion at the end of the pore α-helix that precedes the selectivity filter of the K^+ channel causes loss of K^+ selectivity, Na^+ permeability, and Ca^{2+} influx via opening of voltage-activated T-type Ca^{2+} channels and activation of the Na^+/Ca^{2+} exchange, leading to enhanced CYP11B2 expression and a constitutive over-secretion of aldosterone from the tumor (Choi et al, 2011; Gomez-Sanchez & Oki, 2013).

The prevalence of this novel mutation that was shown to have clearcut consequences, and possible of other unidentified mutations located close to the selectivity filter of KCNJ5 needs to be further investigated. Moreover, whether this novel mutation is associated only with drug-resistant hypertension and/or possibly milder forms of high blood pressure and PA remains to be explored.

Molecular mechanism identified in patients with APAs so far involves mutations of potassium resulting in either membrane depolarization and/or in crease in intracellular calcium (Moraitis et al, 2013). The discovery of new genetic mutations associated with PA has provided fundamental insights into the field of endocrine hypertension. The identification of germ line KCNJ5 mutations in Mendelian forms of endocrine hypertension has advanced our understanding of the pathogenesis of aldosterone-producing adenomas and genetic forms of adrenal hyperplasia, which has important implications for diagnosis and treatment. The genetic basis of more sub-types of PA will likely be identified, and biomarkers for each subtype might become available. We predict that, in the near future, subtype classification of PA will be based on broad genetic and biomarker testing, which will reduce the reliance on AVS for the initiation of targeted therapy.

REFERENCES

REFERENCES

Akerstrom T, Crona J, Delgado Verdugo A, Starker LF, Cupisti K, Willenberg HS, Knoefel WT, Saeger W, Feller A, Ip J, Soon P, Anlauf M, Alesina PF, Schmid KW, Decaussin M, Levillain P, Wangberg B, Peix J-L, Robinson B, Zedenius J, Backdahl M, Caramuta S, Iwen KA, Botling J, Stalberg P, Kraimps J-L, Dralle H, Hellman P, Sidhu S, Westin G, Lehnert H, Walz MK, Akerstrom G, Carling T, Choi M, Lifton RP, Bjorklund P (2012) Comprehensive re-sequencing of adrenal aldosterone producing lesions reveal three somatic mutations near the KCNJ5 potassium channel selectivity filter. *PloS one* 7: e41926

Arnold K, Bordoli L, Kopp J, Schwede T (2006) The SWISS-MODEL workspace: a web-based environment for protein structure homology modelling. *Bioinformatics (Oxford, England)* 22: 195--201

Azizan EAB, Murthy M, Stowasser M, Gordon R, Kowalski B, Xu S, Brown MJ, O'Shaughnessy KM (2012) Somatic mutations affecting the selectivity filter of KCNJ5 are frequent in 2 large unselected collections of adrenal aldosteronomas. *Hypertension* 59: 587-591

Azizan EAB, Poulsen H, Tuluc P, Zhou J, Clausen MV, Lieb A, Maniero C, Garg S, Bochukova EG, Zhao W, Shaikh LH, Brighton CA, Teo AED, Davenport AP, Dekkers T, Tops B, Kusters B, Ceral J, Yeo GSH, Neogi SG, McFarlane I, Rosenfeld N, Marass F, Hadfield J, Margas W, Chaggar K, Solar M, Deinum J, Dolphin AC, Farooqi IS, Striessnig J, Nissen P, Brown MJ (2013) Somatic mutations in ATP1A1 and CACNA1D underlie a common subtype of adrenal hypertension. *Nature genetics* 45: 1055--1060

Bassett MH, Mayhew B, Rehman K, White PC, Mantero F, Arnaldi G, Stewart PM, Bujalska I, Rainey WE (2005) Expression profiles for steroidogenic enzymes in adrenocortical disease. *The Journal of clinical endocrinology and metabolism* 90: 5446--5455

Beuschlein F, Boulkroun S, Osswald A, Wieland T, Nielsen HN, Lichtenauer UD, Penton D, Schack VR, Amar L, Fischer E, Walther A, Tauber P, Schwarzmayr T, Diener S, Graf E, Allolio B, Samson-Couterie B, Benecke A, Quinkler M, Fallo F, Plouin P-F, Mantero F, Meitinger T, Mulatero P, Jeunemaitre X, Warth R, Vilsen B, Zennaro M-C, Strom TM, Reincke M (2013) Somatic mutations in ATP1A1 and ATP2B3 lead to aldosterone-producing adenomas and secondary hypertension. *Nature genetics* 45: 440-444, 444e441-442

Boulkroun S, Beuschlein F, Rossi G-P, Golib-Dzib J-F, Fischer E, Amar L, Mulatero P, Samson-Couterie B, Hahner S, Quinkler M, Fallo F, Letizia C, Allolio B, Ceolotto G, Cicala MV, Lang K, Lefebvre H, Lenzini L, Maniero C, Monticone S, Perrocheau M, Pilon C, Plouin P-F, Rayes N, Seccia TM, Veglio F, Williams TA, Zinnamosca L, Mantero F, Benecke A, Jeunemaitre X,

Reincke M, Zennaro M-C (2012) Prevalence, clinical, and molecular correlates of KCNJ5 mutations in primary aldosteronism. *Hypertension* 59: 592-598

Brenner T, Shaughnessy KMO (2008) Both TASK-3 and TREK-1 two-pore loop K channels are expressed in H295R cells and modulate their membrane potential and aldosterone secretion. *merican Journal of Physiology - Endocrinology and Metabolism* 295: 1480-1486

Brown DR (2005) Neurodegeneration and oxidative stress: prion disease results from loss of antioxidant defence. *Folia neuropathologica / Association of Polish Neuropathologists and Medical Research Centre, Polish Academy of Sciences* 43: 229-243

Brunger AT (2007) Version 1.2 of the Crystallography and NMR system. *Nature protocols* 2: 2728-2733

Calhoun DA, Jones D, Textor S, Goff DC, Murphy TP, Toto RD, White A, Cushman WC, White W, Sica D, Ferdinand K, Giles TD, Falkner B, Carey RM (2008) Resistant hypertension: diagnosis, evaluation, and treatment. A scientific statement from the American Heart Association Professional Education Committee of the Council for High Blood Pressure Research. *Hypertension* 51: 1403-1419

Charmandari E, Sertedaki A, Kino T, Merakou C, Hoffman DA, Hatch MM, Hurt DE, Lin L, Xekouki P, Stratakis CA, Chrousos GP (2012) A Novel Point Mutation in the KCNJ5 Gene Causing Primary Hyperaldosteronism and Early-Onset Autosomal Dominant Hypertension. *The Journal of clinical endocrinology and metabolism* 97: 1--8

Choi M, Ute I S, Peng Y, Peyman B, Bixiao Z, Carol N-W, Weizhen J, Yoonsang C, Aniruddh P, Clara J M, Elias L, Max V W, David S G, Shrikant M, Per H, Gunnar W, Goran A, Wenhui W, Tobias C, Richard P L (2011) K+ channel mutations in adrenal aldosterone-producing adenomas and hereditary hypertension. *Science (New York, NY)* 331: 768-772

Chun J, Fred J S, Gabriel G H (1994) Oxygen Deprivation Activates Substantia Nigra Neurons an ATP-Inhibitable K + Channel. *The Journal of neuroscience* 14: 5590-5602

Conn JW (1955) Presidential address. I. Painting background. II. Primary aldosteronism, a new clinical syndrome. *Journal of Laboratory and Clinical Medicine* 45: 3-7

Conn JW, Louis LH (1956) Primary Aldosteronism, a New Clinical Entity. *Annals of Internal Medicine* 44: 1-15

Corey S (1998a) Identification of Native Atrial G-protein-regulated Inwardly Rectifying K+ (GIRK4) Channel Homomultimers. *Journal of Biological Chemistry* 273: 27499-27504

Corey S (1998b) Number and Stoichiometry of Subunits in the Native Atrial G-protein-gated K+ Channel, IKACh. *Journal of Biological Chemistry* 273: 5271-5278

Dobrev D, Friedrich A, Voigt N, Jost N, Wettwer E, Christ T, Knaut M, Ravens U (2005) The G protein-gated potassium current I(K,ACh) is constitutively active in patients with chronic atrial fibrillation. *Circulation* 112: 3697-3706

Emsley P, Cowtan K (2004) Coot: model-building tools for molecular graphics. *Acta crystallographica Section D, Biological crystallography* 60: 2126-2132

Fink M, Lesage F, Duprat F, Heurteaux C, Reyes R, Fosset M, Lazdunski M (1998) A neuronal two P domain K+ channel stimulated by arachidonic acid and polyunsaturated fatty acids. *The EMBO journal* 17: 3297-3308

G K, E. A G, WICKMAN;, K V, B K, L DE C (1995) The G-protein-gated atrial K+ channel IKAch is a heteromultimer of two inwardly rectifying K+-channel proteins. *Nature* 374: 135-141

Geller DS, Zhang J, Wisgerhof MV, Shackleton C, Kashgarian M, Lifton RP (2008) A novel form of human mendelian hypertension featuring nonglucocorticoid-remediable aldosteronism. *The Journal of clinical endocrinology and metabolism* 93: 3117-3123

Gomez-Sanchez CE, Oki K (2013) Minireview: Potassium Channels and Aldosterone Dysregulation. Is Primary Aldosteronism a Potassium Channelopathy? *Endocrinology*: 1-9

Heitzmann D, Derand R, Jungbauer S, Bandulik S, Sterner C, Schweda F, El Wakil A, Lalli E, Guy N, Mengual R, Reichold M, Tegtmeier I, Bendahhou S, Gomez-Sanchez CE, Aller MI, Wisden W, Weber A, Lesage F, Warth R, Barhanin J (2008) Invalidation of TASK1 potassium channels disrupts adrenal gland zonation and mineralocorticoid homeostasis. *The EMBO journal* 27: 179-187

Hibino H, Inanobe A, Furutani K, Murakami S, Findlay YK (2010) Inwardly Rectifying Potassium Channels : Their Structure , Function , and Physiological Roles. *Physiological Review* 90: 291-366

Jabbari J, Olesen MS, Holst AG, Nielsen JB, Haunso S, Svendsen JH (2011) Common polymorphisms in KCNJ5 corrected are associated with early-onset lone atrial fibrillation in Caucasians. *Cardiology* 118: 116-120

Kuo A, Gulbis JM, Antcliff JF, Rahman T, Lowe ED, Zimmer J, Cuthbertson J, Ashcroft FM, Ezaki T, Doyle DA (2003) Crystal structure of the potassium channel KirBac1.1 in the closed state. *Science (New York, NY)* 300: 1922-1926

Lenzini L, Caroccia B, Campos AG, Fassina A, Belloni AS, Seccia TM, Kuppusamy M, Ferraro S, Skander G, Bader M, Rainey WE, Rossi GP (2013) Lower Expression of the Twik-Related Acid-Sensitive K+ Channel 2 (Task-2) Gene Is a Hallmark of Aldosterone Producing Adenoma Causing Human Primary Aldosteronism. *The Journal of clinical endocrinology and metabolism* 2: 1-9

Lenzini L, Seccia TM, Aldighieri E, Belloni AS, Bernante P, Giuliani L, Nussdorfer GG, Pessina AC, Rossi GP (2007) Heterogeneity of aldosterone-producing adenomas revealed by a whole transcriptome analysis. *Hypertension* 50: 1106-1113

Li N, Zhang D, Zhang J, Guo Y, Yan Z, Wang H, Zhou L, Hong J, Wang X, A Z (2012) Influence of age on the association of GIRK4 with metabolic syndrome. *Annals of clinical biochemistry* 49: 369-376

Litynski M (1953) Hypertension caused by tumors of the adrenal cortex. *Polski tygodnik lekarski (warsaw)*: 204-208

Lucinda A D, Changlong H, Nick A G, Neil Sen XC, Edmund M T, Robert M C, Douglas A B, Paula Q B (2008) TASK channel deletion in mice causes primary hyperaldosteronism Lucinda. *Proceedings of the National Academy of Sciences of the United States of America* 105: 9663-9667

Monticone S, Hattangady NG, Nishimoto K, Mantero F, Rubin B, Cicala MV, Pezzani R, Auchus RJ, Ghayee HK, Shibata H, Kurihara I, Williams TA, Giri JG, Bollag RJ, Edwards MA, Isales CM, Rainey WE (2012) Effect of KCNJ5 mutations on gene expression in aldosterone-producing adenomas and adrenocortical cells. *The Journal of clinical endocrinology and metabolism* 97: E1567-1572

Monticone S, Hattangady NG, Penton D, Isales CM, Edwards MA, Williams TA, Sterner C, Warth R, Mulatero P, Rainey WE (2013) A Novel Y152C KCNJ5 Mutation Responsible for Familial Hyperaldosteronism Type III. *The Journal of clinical endocrinology and metabolism* 98: E1861-1865

Moraitis AG, Rainey WE, Auchus RJ (2013) Gene mutations that promote adrenal aldosterone production, sodium retention, and hypertension. *The application of clinical genetics* 7: 1-13

Mulatero P, Stowasser M, Loh KC, Fardella CE, Gordon RD, Mosso L, Gomez-Sanchez CE, Veglio F, Young WF (2004) Increased diagnosis of primary aldosteronism, including surgically correctable forms, in centers from five continents. *The Journal of clinical endocrinology and metabolism* 89: 1045-1050

Mulatero P, Tauber P, Zennaro MC, Monticone S, Lang K, Beuschlein F, Fischer E, Tizzani D, Pallauf A, Viola A, Amar L, Williams TA, Strom TM, Graf E, Bandulik S, Penton D, Plouin PF, Warth R, Allolio B, Jeunemaitre X, Veglio F, Reincke M (2012) KCNJ5 mutations in European families with nonglucocorticoid remediable familial hyperaldosteronism. *Hypertension* 59: 235-240

Murthy M, Azizan EAB, Brown MJ, O'Shaughnessy KM (2012) Characterization of a novel somatic KCNJ5 mutation delI157 in an aldosterone-producing adenoma. *Journal of hypertension* 30: 1827-1833

Murthy M, Xu; S, Massimo; G, Wolly; M, Gordon; RD, Stowasser; M, O'Shaughnessy KM (2013) A role for germline mutations and a rare coding SNP within the KCNJ5 potassium channel in a large cohort of sporadic cases of Primary aldosteronism. *Hypertension*

Rayner B (2008) Primary aldosteronism and aldosterone-associated hypertension. *Journal of clinical pathology* 61: 825-831

Richard P L, Robert G D, Michael P, Glenn M R, Sandra C, Stanley U, Jean-Marc L (1992) A chimaeric 11β-hydroxylase/aldosterone synthase gene causes glucocorticoid-remediable aldosteronism and human hypertension. *Nature* 355: 261--264

Rossi E, Regolisti G, Negro A, Sani C, Davoli S, Perazzoli F (2002) High Prevalence of Primary Aldosteronism to Renin Ratio as a Screening Test Among Italian Hypertensives. *American Journal of Hypertension* 15: 896--902

Rossi GP, Bernini G, Caliumi C, Desideri G, Fabris B, Ferri C, Ganzaroli C, Giacchetti G, Letizia C, Maccario M, Mallamaci F, Mannelli M, Mattarello M-J, Moretti A, Palumbo G, Parenti G, Porteri E, Semplicini A, Rizzoni D, Rossi E, Boscaro M, Pessina AC, Mantero F (2006a) A prospective study of the prevalence of primary aldosteronism in 1,125 hypertensive patients. *Journal of the American College of Cardiology* 48: 2293-2300

Rossi GP, Bernini G, Desideri G, Fabris B, Ferri C, Giacchetti G, Letizia C, Maccario M, Mannelli M, Matterello M-J, Montemurro D, Palumbo G, Rizzoni D, Rossi E, Pessina AC, Mantero F (2006b) Renal damage in primary aldosteronism: results of the PAPY Study. *Hypertension* 48: 232-238

Rossi GP, Seccia TM, Maniero C, Pessina AC (2011) Drug-related hypertension and resistance to antihypertensive treatment: a call for action. *Journal of hypertension* 29: 2295-2309

Rossi GP, Sechi LA, Giacchetti G, Ronconi V, Strazzullo P, Funder JW (2008) Primary aldosteronism: cardiovascular, renal and metabolic implications. *Trends in endocrinology and metabolism: TEM* 19: 88-90

Scholl UI, Goh G, Stolting G, de Oliveira RC, Choi M, Overton JD, Fonseca AL, Korah R, Starker LF, Kunstman JW, Prasad ML, Hartung EA, Mauras N, Benson MR, Brady T, Shapiro JR, Loring E, Nelson-Williams C, Libutti SK, Mane S, Hellman P, Westin G, Akerström G, Bjorklund P, Carling T, Fahlke C, Hidalgo P, Lifton RP (2013) Somatic and germline CACNA1D calcium channel mutations in aldosterone-producing adenomas and primary aldosteronism. *Nature genetics* 45: 1050-1054

Scholl UI, Lifton RP (2013) New insights into aldosterone-producing adenomas and hereditary aldosteronism: mutations in the K+ channel KCNJ5. *Current opinion in nephrology and hypertension* 22: 141-147

Scholl UI, Nelson-Williams C, Yue P, Grekin R, Wyatt RJ, Dillon MJ, Couch R, Hammer LK, Harley FL, Farhi A, Wang W-H, Lifton RP (2012) Hypertension with or without adrenal hyperplasia due to different inherited mutations in the potassium channel KCNJ5. *Proceedings of the National Academy of Sciences of the United States of America* 109: 2533-2538

Seccia TM, Fassina A, Nussdorfer GG, Pessina AC, Rossi GP (2005) Aldosterone-producing adrenocortical carcinoma: an unusual cause of Conn's syndrome with an ominous clinical course. *Endocrine-related cancer* 12: 149-159

Seccia TM, Mantero F, Letizia C, Kuppusamy M, Caroccia B, Barisa M, Cicala MV, Miotto D, Rossi GP (2012) Somatic mutations in the KCNJ5 gene raise the lateralization index: implications for the diagnosis of primary aldosteronism by adrenal vein sampling. *The Journal of clinical endocrinology and metabolism* 97: E2307-2313

So A, Duffy DL, Gordon RD, Jeske YWA, Lin-Su K, New MI, Stowasser M (2005) Familial hyperaldosteronism type II is linked to the chromosome 7p22 region but also shows predicted heterogeneity. *Journal of hypertension* 23: 1477-1484

Spät A (2004) Glomerulosa cell-a unique sensor of extracellular K+ concentration. *Molecular and cellular endocrinology* 217: 23-26

Stowasser M, Gordon RD (2013) The renaissance of primary aldosteronism: what has it taught us? *Heart, lung & circulation* 22: 412-420

Taguchi R, Yamada M, Nakajima Y, Satoh T, Hashimoto K, Shibusawa N, Ozawa A, Okada S, Rokutanda N, Takata D, Koibuchi Y, Horiguchi J, Oyama T, Takeyoshi I, Mori M (2012) Expression and Mutations of KCNJ5 mRNA in Japanese Patients with Aldosterone-Producing Adenomas. *The Journal of clinical endocrinology and metabolism* 97: 1311-1319

Wang T, Satoh F, Morimoto R, Nakamura Y, Sasano H, Auchus RJ, Edwards MA, Rainey WE (2011) Gene expression profiles in aldosterone-producing adenomas and adjacent adrenal glands. *European journal of endocrinology / European Federation of Endocrine Societies* 164: 613-619

WHO; (1999) Guidlines. *World Health Organization-International Society of Hypertension Guidelines for the management of hypertension Guidelines sub-committee of the World Health Organization*

Wickman K, Pu WT, Clapham DE (2002) Structural characterization of the mouse Girk genes. *Gene* 284: 241-250

Yang Y, Yang Y, Liang B, Liu J, Li J, Grunnet M, Olesen S-P, Rasmussen HB, Ellinor PT, Gao L, Lin X, Li L, Wang L, Xiao J, Liu Y, Liu Y, Zhang S, Liang D, Peng L, Jespersen T, Chen Y-H (2010)

Identification of a Kir3.4 Mutation in Congenital Long QT Syndrome. *The American Journal of Human Genetics* 86: 872-880

Zagotta WN (2006) Permutations of permeability. *Nature* 440: 427-429